

The Role of $ERR\alpha$ in Dictating the Hepatic Metabolic Response to Dietary Sugars,
Fructose and Glucose

Christina-Angela Guluzian

Department of Biochemistry

McGill University, Montréal

December 2022

A thesis submitted to McGill University in partial fulfillment of requirements of the degree
of Master's of Science

© Christina-Angela Guluzian 2022

I. ABSTRACT	4
II. RÉSUMÉ	6
III. ACKNOWLEDGEMENTS.....	8
IV. CONTRIBUTIONS OF AUTHORS.....	9
V. LIST OF ABBREVIATIONS.....	11
VI. LIST OF FIGURES	13
VII. METHODS	14
VIII. INTRODUCTION	16
IX. LITERATURE REVIEW	18
1) Non-Alcoholic Fatty Liver Disease	18
1.1 Natural History of Fatty Liver Disease.....	18
1.2 The “Two Hit Model” does not hit all bases.....	19
1.3 Type 2 Diabetes and NAFLD.....	20
1.3.1 T2DM and NAFLD Prevalence.....	20
1.3.2 The Selective Insulin Resistance Hypothesis	20
1.3.3 Canonical Insulin Signaling	21
1.3.4 Hepatic Insulin Resistance	22
1.3.5 Skeletal Muscle Insulin Resistance.....	23
1.3.5.1 Muscle Glycogen to Hepatic Fat	23
1.3.5.2 Exercise restores proper carbohydrate metabolism in muscle	24
1.3.6 Adipose Tissue Insulin Resistance.....	24
1.3.6.1 Lipolysis.....	24
1.3.6.2 Ectopic Fat Distribution and Quantity.....	25
1.4 Lifestyle Management to Improve NAFLD and T2DM	26
2) Glucose and Fructose Metabolism.....	27
2.1 Epidemiological Trends in Sugar Consumptions	27
2.2 Divergent Fructose and Glucose Metabolism	28
2.2.1 Organismal Level: Gut-Liver Axis.....	29
2.2.1.1 Sugar Transporters GLUT5 and SGLT1	29
2.2.1.2 Absorption throughout the GI tract	29
2.2.1.3 Circulating Levels of Fructose and Glucose	30
2.2.2 Cellular Fructolysis vs Glycolysis in Hepatocytes.....	30
2.2.2.1 Hexokinases KHK and GCK.....	30

2.2.2.2 Fructose metabolite F1P as signaling molecule	31
2.2.2.3 Convergence below PFK.....	31
2.3 Fructose Metabolism in NAFLD and T2DM	31
2.3.1 Increased De Novo Lipogenesis	31
2.3.2. Transcriptional Regulation: ChREBP and SREBP-1c.....	32
2.3.3. Decreased Fatty Acid Oxidation.....	33
3. Nuclear Receptors	33
3.1 Transcriptional Regulation of Energy Homeostasis.....	33
3.2 The Estrogen Related Receptors	34
3.3 Structure of the ERRs	35
3.3.1 Amino Terminal Domain	35
3.3.2 DNA Binding Domain.....	35
3.3.3 Ligand Binding Domain.....	36
3.4 ERR α Regulation.....	36
3.4.1 Co-Activator PGC-1 α	37
3.4.2 Co-Repressors NCoR1, PROX1 and NRIP	38
3.5 The Role of ERR α in Energy Metabolism	39
3.5.1 ERR α Transcriptomic Studies	39
3.5.2 Phenotype of the ERR α mouse models.....	40
3.6 Contributions to Metabolic Disease.....	42
3.6.1 Glucose Metabolism and Insulin Resistance	42
3.6.2 Lactate Metabolism.....	44
3.6.3 Lipid Utilization.....	44
3.6.4 Mitochondrial Biogenesis, Fusion and Fission.....	45
3.7 ERR α as a metabolic transcriptional hub.....	45
X. RESULTS	47
XI. FIGURES	54
XII. DISCUSSION	69
XIII. CONCLUSION.....	75
REFERENCES.....	76

I. ABSTRACT

Over the past 40 years, increased consumption of sucrose and high fructose corn syrup (HFCS) in sweetened beverages has paralleled the rising incidence of obesity, diabetes and NAFLD in Canadians. In addition to a variety of external lifestyle factors, it is known that increased caloric intake and decreased energy expenditure are the prime risk factors for metabolic diseases. However, in recent years it has become of interest to investigate if the type of food ingested also has an effect on the development of metabolic disorders. HFCS and sucrose are composed of sugar monomers, glucose and fructose, two six membered carbon rings that have vastly different metabolic fates in the body. Identification of the dietary sugar fructose as being responsible for not only the formation of body fat in mice, but also the decrease in hepatic transcriptional pathways involved in fatty acid oxidation, has highlighted the additive negative effects of this sugar, particularly in the context of a high-fat diet (HFD). Mice fed this high-fat, high-fructose diet display mitochondrial dysfunction and an upregulation of the master regulator of mitochondrial biogenesis, peroxisome proliferator-activated receptor-gamma coactivator (PGC-1 α). Members of the PGC-1 co-activator family have been extensively linked to the transcriptional activities of another well-known group of metabolic regulators, the estrogen-related receptors (ERRs). In particular, PGC-1 α has been described as a protein ligand used to fine tune the transcriptional activity of ERR α in response to physiological stimuli such as cold exposure, exercise or caloric restriction. As such, we hypothesize that fructose could be another external modulator of the ERR α /PGC-1 α transcriptional axis and sought to detangle the role of the nuclear receptor ERR α in this process. An ERR α knockout model (ERR $\alpha^{-/-}$) conferring loss of function and another model harboring mutations to three ERR α phosphosites (ERR α^{3SA}) causing an overabundance of protein, were used to detangle ERR α 's involvement in the hepatic metabolic response to fructose consumption. Male mice were subjected to a low-fat control diet (LFD) or a diet containing 60% calories from fat (HFD), supplemented with water, 30% (w/v) glucose or 30% (w/v) fructose solutions for 10 weeks. Male ERR α mice were used instead of females, because in previous metabolic studies this sex displayed increased vulnerability to metabolic insults like

HFDs, thus making them ideal for this study. Overall, loss of $ERR\alpha$ in mice fed a HFD supplemented with glucose caused significantly less weight gain, despite increased caloric intake as compared to just a HFD. These mice seemed to be protected from diet induced obesity, hepatic steatosis, and glucose intolerance, as they showed decreased adipose tissue mass, liver weights and lowered fasting glucose levels with improved glucose clearance during a GTT. Supplementation with fructose in $ERR\alpha^{-/-}$ fed a HFD did not deviate significantly from WT controls. Conversely, overabundance of $ERR\alpha$ protein expression in mice fed a HFD supplemented with fructose, showed a similar protective phenotype, highlighting a possible divergent role for $ERR\alpha$ in the glucose and fructose metabolism. Lastly, $ERR\alpha^{3SA}$ mice fed a HFD supplemented with glucose were also similar to WT. Overall, these results are compatible with our current understanding of $ERR\alpha$ regulating genes involved in lipid utilization, insulin sensitivity, and mitochondrial function but the observation that its loss and overabundance protects against excess glucose and fructose consumption, respectively, was novel and thus merits further investigation.

II. RÉSUMÉ

Au cours des 40 dernières années, l'augmentation de la consommation de saccharose et de sirop de maïs riche en fructose dans les boissons sucrées parallèle l'augmentation de l'incidence de l'obésité, du diabète et de la stéatose hépatique non alcoolique (NAFLD) dans les Canadiens. Plusieurs facteurs externes relient notre mode de vie au développement des maladies métaboliques, mais on sait en général que l'augmentation de la consommation calorique et la diminution de la dépense énergétique sont un risque majeur. Cependant, il est devenu intéressant ces dernières années de rechercher si le type d'aliment ingéré a également un effet sur le développement de troubles métaboliques. Le HFCS et le saccharose sont composés de monomères de sucre, glucose et fructose, deux molécules de six carbones qui ont des destins métaboliques très différents dans le corps. L'identification que le fructose est responsable pour la formation de graisse corporelle et aussi pour la diminution des voies transcriptionnelles hépatiques impliquées dans l'oxydation des acides gras dans les souris a mis en évidence les effets négatifs additifs de ce sucre, notamment dans le cadre d'un régime riche en matières grasses. Des souris nourries avec ce régime riche en graisses et en fructose présentent un dysfonctionnement mitochondrial et une expression élevée du régulateur principal de la biogenèse mitochondriale, le coactivateur du récepteur activé par les proliférateurs de peroxysomes gamma ($PGC-1\alpha$). La famille des co-activateurs $PGC-1$ a été largement liée aux activités transcriptionnelles d'un autre groupe bien connu de régulateurs métaboliques, les récepteurs liés aux œstrogènes (ERRs). En particulier, $PGC-1\alpha$ a été décrit comme un ligand protéique utilisé pour affiner les activités transcriptionnelles d' $ERR\alpha$ en réponse à des stimuli externes comme l'exposition au froid, l'exercice ou la restriction calorique. Nous avons émis l'hypothèse que le fructose pourrait être un autre modulateur externe de l'axe transcriptionnel $ERR\alpha/PGC-1\alpha$, et cherchons donc à élucider le rôle du récepteur nucléaire $ERR\alpha$ dans ce processus. Un modèle de knock-out $ERR\alpha$ ($ERR\alpha^{-/-}$) conférant une perte de fonction et un autre modèle hébergeant des mutations de trois phosphosites dans $ERR\alpha$ ($ERR\alpha^{3SA}$) provoquant la stabilisation constitutive de la protéine, ont été utilisés pour éclaircir l'implication d' $ERR\alpha$ dans la réponse métabolique hépatique à la

consommation de fructose. Des souris mâles ont été soumises à un régime témoin pauvre en graisses ou à un régime riche en graisses à 60 %, additionné d'eau, de glucose à 30 % ou de fructose à 30 % pendant 10 semaines. Dans l'ensemble, la perte d'ERR α chez les souris nourries avec un HFD complété par du glucose a entraîné une prise de poids significativement moindre, malgré une augmentation de l'apport calorique par rapport à un HFD seul. Ces souris semblaient être protégées contre l'obésité induite par une diminution du poids et de la stéatose hépatique et une tolérance au glucose améliorée, car ces souris présentaient une diminution de la masse du tissu adipeux et du poids du foie et une diminution de la glycémie à jeun avec une amélioration de la clairance du glucose pendant un test de tolérance au glucose. À l'inverse, la surabondance de l'expression de la protéine ERR α chez les souris nourries avec un HFD supplémenté en fructose, a montré un phénotype protecteur similaire, mettant en évidence un rôle divergent possible pour ERR α dans le métabolisme du glucose et du fructose. Dans l'ensemble, le projet est conforme à la littérature précédente et à notre compréhension des gènes régulateurs de l'ERR α impliqués dans l'utilisation des lipides, de la sensibilité à l'insuline et de la fonction mitochondriale, mais l'observation que sa perte et sa surabondance protègent respectivement contre la consommation excessive respective de glucose et de fructose sont nouvelles et méritent une recherche plus approfondie.

III. ACKNOWLEDGEMENTS

First and foremost, I would like to thank my supervisor Dr. Vincent Giguère for providing me with a wonderful opportunity to pursue this project, as well as giving his unwavering support and encouragement throughout my Master's degree. My lab mates, Dr. Charlotte Scholtes, Catherine Rosa Dufour, Majid Ghahremani, Dr. Hui Xia, Dr. Younes Medkour, Stephanie Han and Dr. Ting Li, for keeping me motivated and sane. I would also like to thank the members of my Research Advisory Committee, Dr. Lawrence Kazak and Dr. Jennifer Estall, for their constructive feedback and guidance. I am also thankful for my two best and brightest friends, Tara Shomali and Emma Wilson, who know me better than myself and encouraged me to persevere at my lowest moments. To my oldest and dearest friend, Sarah Milton, thank you, for reminding me to not take things too seriously, because at the end of the day "we are all on a floating rock anyways". Lastly, I would like to give my biggest thanks to my parents and brother, who gave me the skills and courage to take on this expedition.

IV. CONTRIBUTIONS OF AUTHORS

I confirm that I, Christina Guluzian, unless stated otherwise, have performed the experiments outlined in this manuscript. Additionally, I have analyzed the data and drafted this thesis with editorial comments and corrections made by Dr. Vincent Giguère. Some of the contributions below were done during my thesis but complete data has not been received back in time for the drafting of the manuscript.

Processing of Tissues for Staining

Paraffin-embedding, sectioning, H&E and Oil Red O staining was performed by the Histology Core at the Goodman Cancer Institute.

Electron Microscopy Sectioning and Training

I was trained by Chief Electron Microscopy Technician, Johanne Ouellette, at the Facility of Electron Microscopy Research (FEMR) to embed liver tissues in epon. Following this, sectioning and loading on of samples onto EM grids were performed by Johanne Ouellette. Imaging using Tecnai[™] Spirit Electron Microscope will be done by myself to visualize liver mitochondrial size and number.

Tissue Dissection and Animal Handling

Tissue dissection of liver, iWAT, eWAT, gastrocnemius and soleus muscle, in addition to glucose readings taken at the time of sacrifice, were performed by me and one other lab member depending on availability. Contributing members included Dr. Charlotte Scholtes, Catherine Rosa Dufour and Carlo Ouellet. A significant amount of additional aid was done by our animal technician, Carlo Ouellet to breed, tag and genotype mice for this project, as well as aiding with GTT and ITT tests.

Mouse Models

There were two mouse models used in this manuscript, with an additional wildtype control model. The ERR α knockout model, produced in 1997 by the Giguère's lab, was made by swapping an exon in the amino terminal domain with a neo^r cassette. This full

body knockout is well characterized in literature and the lab and contains no $ERR\alpha$ isoform. The second, newer mouse model, was produced by (previous) PhD student Dr. Hui Xia. The $ERR\alpha^{3SA}$ phosphomutant mouse was generated on a C57BL/6N genetic background using CRISPR/Cas9 gene editing. Three serine residues (S19, S22 and S26) are phosphorylated on the amino-terminal domain (NTD) of $ERR\alpha$, which causes its subsequent ubiquitination and degradation in the proteasome. Thus, three serine to alanine point mutations were made to these locations using CRISPR/Cas9 gene editing, protecting the receptor from phosphorylation and UPS mediated degradation, thus resulting in the overabundance of the protein. These two mouse strains represent gain and loss of function models of $ERR\alpha$ activity used in this project.

V. LIST OF ABBREVIATIONS

ACACA	Acetyl-CoA carboxylase
AF2	Activation function-2
ALDOB	Aldolase B
ATP	Adenosine triphosphate
Acss2	Acetyl-CoA synthetase
C29	Compound 29
CPT1	Carnitine palmitoyltransferase 1
ChREBP	Carbohydrate response element-binding protein
ChIP	Chromatin Immunoprecipitation
DAGs	Diacylglycerol
DBD	DNA Binding Domain
DHAP	Dihydroxyacetone phosphate
DNL	de novo lipogenesis
ERR α	Estrogen related receptor α
ERR α ^{3SA}	ERR α phosphomutant (S19A S22A S26A)
ER α	Estrogen receptor α
ERRE	ERR response element
F1P	Fructose-1-phosphate
FA	Fatty acid
FAO	Fatty acid oxidation
FFAs	Free fatty acid
G3P	Glyceraldehyde-3-phosphate
G6P	Glucose 6-phosphate
GCK	Glucokinase
GCKR	Glucokinase regulatory protein
GCN5	General control non-depressible 5
GTT	glucose tolerance test
Gastro	gastrocnemius
H&E	Hematoxylin and eosin

HCC	hepatocellular carcinoma
HDAC8	Histone deacetylase 8
HFCS	High fructose corn syrup
HFD	High Fat Diet
IL6	Interleukin 6
IP	Intraperitoneal
ITT	Insulin tolerance test
KHK	Ketohexokinase
LBD	Ligand Binding Domain
LDH	Lactate dehydrogenase
LFD	Low Fat Diet
LKO-ERR α	Liver Knockout Estrogen Related Receptor α
MFN1/2	Mitofusin 1/Mitofusin 2
Min	Minutes
NAFLD	Non-Alcoholic Fatty Liver Disease
NASH	Nonalcoholic steatohepatitis
NR	Nuclear receptor
NRF1/2	Nuclear Respiratory Factor 1/2
NTD	Amino Terminal Domain
OPA1	Optic Atrophy 1
ORO	Oil Red O
OXPPOS	Oxidative Phosphorylation
PCAF	P300/CBP-associated factor
PDK4	Pyruvate Dehydrogenase Kinase 4
PEPCK	Phosphoenolpyruvate carboxykinase
PFK	Phosphofructokinase-1
PGC-1 α	Peroxisome proliferator-activated receptor gamma coactivator 1- α
PKC ϵ	Protein kinase C
RNA-seq	RNA sequence
SGLT1	Sodium-glucose linked transporter 1
SREBP1	Sterol regulatory element-binding transcription factor 1

Sirt1	Sirtuin 1
Sol	Soleus
TCA	Tricarboxylic acid
TFAM	Transcription factor A, mitochondrial
TFB1M/TFB2M	Transcription Factor B1, Mitochondrial
TGs	Triglycerides
TKFC	Triokinase And FMN Cyclase
VLDL	Very-low-density lipoprotein
eWAT	epididymal White Adipose Tissue
iWAT	inguinal White Adipose Tissue

VI. LIST OF FIGURES

Figure A: Schematic experimental setup

Figure B: The Natural History of Fatty Liver disease

Figure C: Insulin Resistance manifests due to cross talk between liver, skeletal muscle and adipose tissue.

Figure D: Structure and Interactions of ERR α

Figure E: In vivo models for ERR α activity

Figure 1: Sugar Consumption on a HFD induces divergent weight gain patterns in ERR $\alpha^{-/-}$, ERR α^{3SA} and WT mice

Figure 2: Diet-induced weight changes in liver, adipose tissue and skeletal muscle in ERR $\alpha^{-/-}$, ERR α^{3SA} and their wildtype controls.

Figure 3: Diet-induced changes in gross liver appearance in ERR $\alpha^{-/-}$, ERR α^{3SA} and their wildtype controls.

Figure 4: Diet-induced changes in lipid distribution in ERR $\alpha^{-/-}$, ERR α^{3SA} and their wildtype controls.

Figure 5: Diet-induced changes in glucose homeostasis in ERR $\alpha^{-/-}$, ERR α^{3SA} and their wildtype controls.

Figure 6: Diet-induced changes in insulin homeostasis in ERR $\alpha^{-/-}$, ERR α^{3SA} and their wildtype controls.

Figure 7: Flow chart summarizing comparisons of diet induced changes between WT, $ERR\alpha^{-/-}$ and $ERR\alpha^{3SA}$ mice.

Table 1: Total (pellet and liquid) weekly caloric (kcal) consumption per mouse.

Table 2: Liver and adipose tissue weights per diet condition.

VII. METHODS

Mice

All mouse experimental procedures were approved and followed by the McGill University Animal Care Committee and in compliance with the guidelines of the Canadian Council on Animal Care (Protocol #3173). All experiments used male mice of around 5-6 weeks of age. Mice were housed 2-5 per cage in standard continuous conditions; at ambient temperature of 18-24°C, relative humidity of 30-70% and under a 12-hour light-dark cycle (7am-7pm light, 7pm-7am dark). Back crossing was performed thrice with C57BL/6NHsd wildtype mice (Envigo) with the two $ERR\alpha$ mouse models used in this experiment to ensure minimization of genetic background variance. Backcrossed heterozygous (+/-) transgenic mice ($ERR\alpha^{-/-}$ or $ERR\alpha^{3SA}$) were mated backcrossed homozygous (-/-) transgenic mice to generate the appropriate (-/-) homozygous pups used for experiments. For genotyping, genomic DNA was isolated from tail samples and were amplified by polymerase chain reaction (PCR).

Diets

Mice were allowed *ad libitum* access to a 60% High Fat Diet (HFD; Research diets; D12492; 5.24 kcal/g; 60 kcal% fat, 20 kcal% protein, 20 kcal% carbohydrates) or to a sucrose matched, Low Fat Diet control (LFD; Research diets; D12450J; 3.85 kcal/g; 10 kcal% fat, 20% kcal protein, 70% kcal carbohydrates). Additionally, mice were supplied with either tap water, a 30% (weight/volume) fructose solution or 30% glucose solution in 250 mL water bottles (prepared day of). Mice were weighed weekly and food and liquid intake were measured at the same time.

Sacrifice Techniques

After 10 weeks on their respective diets, mice were sacrificed by cervical dislocation Zeitgeber time (ZT) 2–6 for serum and tissue collection. Blood was collected into Eppendorf tube right before sacrifice from the submandibular vein, punctured using a 24G needle. Serum was obtained by spinning sample down in microcentrifuge at 5000 rpm for 30 minutes to isolate the plasma. This blood was also used to measure circulating glucose (OneTouch Ultra[®]2 glucose meter, OneTouch Ultra Glucose strips) and lactate (Lactate Scout+ meter, Lactate Scout Test Strips) measurements. Following cervical dislocation, liver, skeletal muscle (gastrocnemius and soleus), epididymal and inguinal white adipose tissue were harvested, weighed and snap frozen in liquid nitrogen and subsequently stored at -80°C to await processing. Tissue samples were also taken at this time for histological staining.

Glucose and Insulin Tolerance Tests

One week prior to either glucose tolerance test (GTT) or insulin tolerance test (ITT), mice were transferred from cornchip to woodchip bedding cages. At 8 weeks of age, mice were selected at random to either undergo an ITT or GTT. For the GTT tests, mice were fasted, with free access to water, for 12 hours prior to the beginning of the first injection. Cages placed under a heat lamp for 20-30 minutes before the beginning of the test for an acclimation period, mice were weighed individually, and a basal fasting blood glucose was taken. A 20% D-glucose (cat. no. 15023-021; Thermo Fisher Scientific) solution in 0.9% NaCl was prepared and sterilized with 0.22 µm filter. Based on whole body weight, intraperitoneal injections (IP) at 2 g/kg were performed. The circulating blood glucose measurements were recorded using glucometer (OneTouch Ultra[®]2 glucose meter) at 0, 15, 30, 60, and 120 minutes after injection via the lateral tail vein. If more than one cage was to undergo a tolerance test in one day, mice were injected in alternation between cages.

For ITT tests, mice were fasted for 3 hours prior to first injection. LFD and HFD mice received insulin (cat. no. I0516-5 ml; Sigma-Aldrich) injections of 0.75 U/kg or 2 U/kg, respectively. Blood glucose measurements were subsequently monitored similarly over the next 2 hours.

VIII. INTRODUCTION

Nuclear receptors are a class of transcription factors whose main function is to integrate external stimuli into specific changes in gene expression within the cell. Nuclear receptors are responsible for a large range of physiological processes such as development, homeostasis and metabolism. In response to ligands such as hormones, vitamins, drugs and metabolites, nuclear receptors will move to the genome and bind DNA directly to regulate gene expression. This project will focus on how the orphan nuclear receptor, $ERR\alpha$, transcriptionally regulates fatty acid metabolism in the liver, in response to a high fat diet supplemented with the two most commonly consumed sugars, glucose and fructose. Previous studies done in mice has shown that a HFD supplemented with fructose not only promotes an excess accumulation of body fat but also prevents fatty acid oxidation, resulting in obesity and insulin insensitivity. One node of regulation that these sugars exploit in order to modify fatty acid metabolism is through the master regulator of mitochondrial biogenesis, a protein called $PGC-1\alpha$. As a result, mice subjected to a diet high in fat with high fructose intake, have altered mitochondrial number, function and morphology. However, the underlying biochemical mechanism by which these sugars regulate $PGC-1\alpha$ remains unclear. Important to note, is that $ERR\alpha$'s transcriptional activity is highly diverse, and it relies on a number of co-repressors and activators to regulate a wide range of genes involved in energy metabolism, more specifically lipid and carbohydrate metabolism, pathogen resistance, cancer development and mitochondrial function. In the case of $PGC-1\alpha$, it is a known co-activator of $ERR\alpha$. The hypothesis of this project proposes that, as a central regulator of energy metabolism, $ERR\alpha$ is mechanistically implicated in the hepatic metabolic response to dietary sugars such as fructose and glucose on a diet high in fat.

The aim of this project was to characterize phenotypic changes seen in loss- and gain-of-function mouse models for $ERR\alpha$ activity (referred to as $ERR\alpha^{-/-}$ and $ERR\alpha^{3SA}$) in response to diets rich in fat and certain dietary sugars (i.e. fructose vs glucose) for 10 weeks (Fig. A). These mice (male only) will be monitored to observe if they progress into obesity, NAFLD or develop insulin resistance, which are common in diets high in fat

and fructose. After 8 weeks on their respective diets, their glucose tolerance and insulin sensitivity were measured via glucose tolerance test or insulin tolerance test. Increased areas under the curve for both of these tests corresponds to a worse overall metabolic phenotype. At experimental endpoint, the livers, adipose tissue and skeletal muscle were harvested and weighed to assess how and where these mice were gaining weight, as excess lipid storage in certain organs leads to insulin resistance. Overall, this study sought to establish fructose as a new external nutrient modulator of $ERR\alpha$'s hepatic transcriptional activity and better understand if it plays a pathological or physiological role in the development of diet induced metabolic diseases.

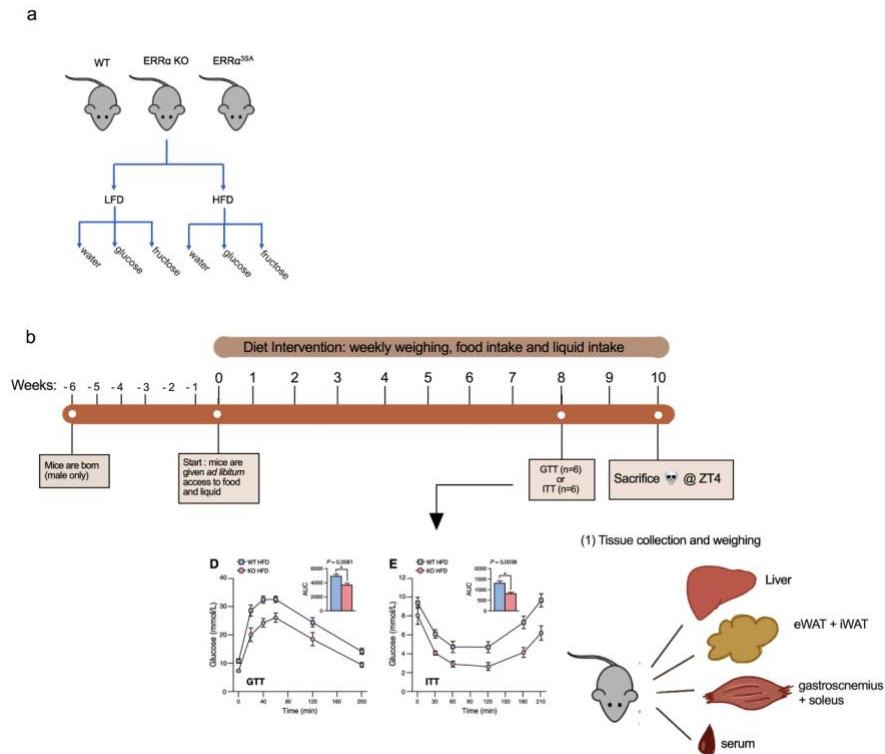


Figure A: Schematic experimental setup. Starting at 6 weeks of age, male $ERR\alpha^{-/-}$, $ERR\alpha^{3SA}$ and WT mice were fed a low fat control diet (LFD), or a sucrose matched 60% high fat diet (HFD), supplemented with regular water, 30% glucose solution or 30% fructose solution (a,b). Mice were weighed weekly and food and liquid intake were also measured. At 8 weeks, glucose and insulin homeostasis was assessed by a GTT or ITT test. At 10 weeks of age, mice were sacrificed from ZT 2–6 and liver, epididymal white adipose tissue (eWAT), inguinal adipose tissue (iWAT), gastrocnemius and soleus muscle were dissected, weighed and snap frozen. n=8-12 per condition. WT, wildtype; KO, $ERR\alpha^{-/-}$; 3SA, $ERR\alpha^{3SA}$

IX. LITERATURE REVIEW

1) Non-Alcoholic Fatty Liver Disease

1.1 Natural History of Fatty Liver Disease

Non-alcoholic fatty liver disease (NAFLD) is the most common chronic liver disease in the western world¹. Its prevalence has slowly been rising since its identification as a clinical entity in 1980 in parallel with other comorbid metabolic diseases such as obesity and type 2 diabetes². Although the term 'NAFLD' has been used as a catch all phrase for a broad spectrum of liver disorders varying in severity, it can be most simply defined by a progressive excess buildup of triglycerides (TG) within the liver, a state called 'steatosis', with the absence of primary causes such as excessive alcohol intake and hepatitis C³. There are benign physiological states where the liver does accumulate moderate amounts of fat, for example during long periods of fasting in which hepatic glycogen storages are spent⁴. In these circumstances visceral body fat will undergo lipolysis to continue supplying lipids to the liver for additional energy, but this acute accumulation of fat within the liver is almost entirely cleared upon refeeding⁴. In contrast, steatosis is defined as having 5.5% of the liver parenchyma occupied by fat, chronically³.

Startlingly, hepatic steatosis is estimated to now be found in 33% of adult livers and 16% of children^{3,5}. In 12-40% of individuals with steatosis, additional inflammation and fibrosis (scarring) will develop in the liver, qualifying them as non-alcoholic steatohepatitis (NASH) patients⁶. During this inflammatory process, resident hepatic stellate cells will transdifferentiate into activated myofibroblasts, and begin to deposit fibrotic tissue in the extra cellular matrix in order to protect hepatocytes^{7,8}. Clinical and experimental evidence has proven that this process is reversible if the underlying etiological agent is removed⁹⁻¹¹. However, NASH is still considered more deleterious than NAFLD, as increased macrophage activation, production of inflammatory cytokines, reactive oxygen species (ROS) accumulation, hepatocyte ballooning and fibrosis all contribute to the parenchyma functioning sub-optimally. NASH is often termed the silent liver disease, as patients with this condition might only experience symptoms years after development, at which point, it may already be too late to treat¹².

The next stage of liver disease is cirrhosis, which occurs in around 25% of NASH patients³. As decades of fibrous septae production accumulate in the liver, this scar tissue will continue to spread and disrupt the functional liver architecture permanently⁸. This damage reduction mechanism tilts homeostasis into a pathological state at which point other organ systems, such as the kidneys and CNS start to be affected⁸.

Although the most common cause of hepatocellular carcinoma (HCC) is hepatitis B & C, cirrhosis caused by progressive NAFLD presents as an additional vital risk factor¹³. The first indication that inflammation was linked to cancer was proposed in 1863 by Rudolph Virchow and was later cemented into the seminal theory on The Hallmarks of Cancer by Hanahan and Weinberg^{14,15}. It is no surprise then that neoplastic HCC lesions usually originate in the chronic inflammatory environment that cirrhosis precedes with¹⁶. Although the hepatocytes are mainly responsible for metabolizing sugar and fat within the liver, other nonparenchymal cells such as the stellate cells, Kueppfer cells and some endothelial cells contribute to disease progression as well.¹⁶ It is thought that the persistent inflammatory response produced by resident nonparenchymal cells and infiltrating immune cells result in oxidative DNA damage and genomic alterations that make conditions favorable for cancer cell to appear¹⁶.

1.2 The “Two Hit Model” does not hit all bases

In 1998, Day and James first described the natural history of NAFLD in the “Two Hit” model, in which steatosis then inflammation characterized major stepping stones in disease progression¹⁷. Despite the diverse histological and imaging staging techniques capable of segregating the sequential progression of a fatty liver to NASH, then cirrhosis and possibly HCC, there remains a large gap of knowledge in our understanding of the molecular mechanisms that drive disease progression or how comorbid conditions contribute to its development (Fig. B)¹⁸. It is generally understood that multiple pathways mechanisms are involved in the pathogenesis such as insulin resistance, obesity, genetic polymorphisms, dietary factors and altered gut microbiota¹⁸.

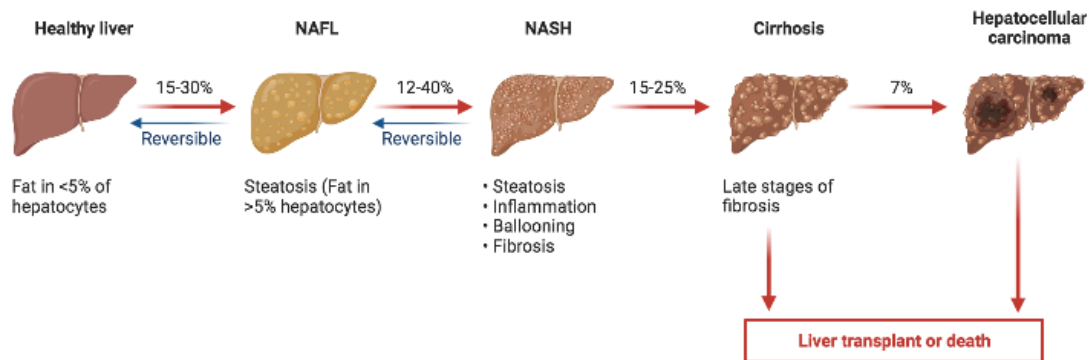


Figure B: The Natural History of Fatty Liver disease. A healthy liver contains approximately 5% fat within hepatocytes. Progressive steps in the pathogenesis of fatty liver disease, such as steatosis to produce NAFLD and inflammation to push further into NASH, increase the chances of a non-reversible phenotype. Cirrhosis is the committed step on this track, which provides a underlying bed of chronic inflammation for cancerous lesions to develop in hepatocellular carcinoma (HCC). Image was produced using Biorender.

1.3 Type 2 Diabetes and NAFLD

1.3.1 T2DM and NAFLD Prevalence

The liver is the center point in the regulation of glucose and lipid metabolism.¹⁸ As such, it is not entirely surprising that there is a strong bidirectional relationship between Type 2 Diabetes (T2DM) and NAFLD¹⁸. NAFLD has a high risk for impaired fasting glucose, an indicator of early diabetes, and conversely approximately 70% T2DM patients will experience some degree of fatty liver disease¹⁸. A long term follow up study of 129 patients with liver biopsy-proven NAFLD showed that 69 of 88 patients had developed insulin resistance, impaired glucose tolerance and fibrosis¹⁹. This finding highlights that although NAFLD usually precedes insulin resistance and T2DM, once developed these secondary metabolic risk factors increase the risk progression of NASH, cirrhosis and even HCC^{19,20}.

1.3.2 The Selective Insulin Resistance Hypothesis

Following a meal rich in carbohydrates, blood glucose levels rise and stimulate the beta cells within the pancreas to release insulin, thereby shifting the body into an

anabolic, energy-storing state^{18,21}. Normal insulin secretion causes glucose uptake by various tissues, whilst suppressing endogenous glucose production and stimulating *de novo lipogenesis* (DNL) in the liver, effectively maintaining a homeostatic range of blood glucose in the body post prandially²². Insulin resistance, a key risk factor for T2DM, can be defined by the inability of key insulin-sensitive tissues, like the liver, skeletal muscle and adipose tissue, to respond and uptake circulating blood glucose for energy (Fig. C)²¹. Additionally, it must be noted, that DNL is paradoxically preserved in both insulin sensitive and insulin resistance livers^{23,24}. This “selective insulin resistance” hypothesis posits that insulin action in this case is still driving DNL, while failing to suppress gluconeogenesis, resulting in hyperglycemia and increased triglyceride production^{23,24}. Common consensus on this phenomenon agrees that it is due to bifurcation of insulin signaling in glucose and lipid metabolism^{23,24}. Thus, it is important to review how these two macromolecules are normally metabolized.

1.3.3 Canonical Insulin Signaling

In a healthy setting, the canonical insulin signaling pathway in the liver requires the coordinated action of several proteins to ultimately result in the suppression of hepatic glucose production (gluconeogenesis) and increase in glycogen synthesis²⁵. When insulin binds and activates its receptor, a tyrosine kinase (IRTK), this results in the phosphorylation and activation of a downstream kinase known as Akt. This kinase then suppresses endogenous glucose production by the liver in two ways²⁶. Firstly, Akt phosphorylates the forkhead box protein FOXO1, a transcription factor, excluding it from the nucleus and preventing it from inducing the expression of the key gluconeogenic enzymes phosphoenolpyruvate carboxykinase (PEPCK) and glucose-6 phosphatase (G6Pase)²⁶. Next, Akt also inactivates glycogen synthase-3 β (GSK3 β) leading to active forms of glycogen synthase kinase (GS), and ultimately, more glycogen production²⁶. These two nodes of modulation, decreased gluconeogenesis and increased glycogen storage, allows insulin action in the liver to efficiently store carbohydrates post-prandially²⁶.

1.3.4 Hepatic Insulin Resistance

In the setting of hepatic insulin resistance, which is marked by the inability of insulin to decrease gluconeogenesis or induce glycogen production, these two arms of modulation have failed, and the liver will still produce glucose²⁶. Studies in mice and humans have shown that the mechanism of lipid-induced hepatic insulin resistance revolves around the action of diacylglycerol (DAG) triggering protein kinase C epsilon (PKC ϵ)²⁷. Samuel et al. showed that increases in hepatic DAG content led to activation of PKC ϵ , which in turn phosphorylates an evolutionarily conserved threonine residue present in the catalytic domain of IRTK^{28,29}. The role of phosphorylation on this threonine residue (T1160) was found to abolish IRTK signaling, through mutation to alanine (T1160A) in mice²⁸. After several days of HFD feeding, a euglycemic clamp, which consists of a steady rate of IV infused insulin and a maintained blood glucose of approximately 100mg/dL by variable infusions, showed that *Insr*^{T1160A} mice remained insulin sensitive, as reflected by a normal ability of insulin to suppress hepatic glucose production during a euglycemic clamp, which is considered the gold standard of measuring insulin sensitivity in humans and mice²⁸. The anti-insulin actions of DAGs and role of lipid induced hepatic insulin resistance seems to have stemmed from an evolutionary need³⁰. During starvation, the fat stored in white adipose tissue undergoes lipolysis to provide energy to the liver once glycogen storages have depleted³⁰. This in turn leads to increased hepatic lipid accumulation (FAs) that need to be stored in their non-lipotoxic form, TAGs.³⁰ Along the pathway of this transformation, three FA chains are connected to a glycerol backbone consecutively, with two chains representing the DAGs.³⁰ As FAs acid delivery through this pathway increases through chylomicron delivery from the blood, de novo lipogenesis or through the diet, this increases DAG content and activates PKC ϵ 's phosphorylation of IRTK's T1160 residue, thus preventing insulin stimulated utilization of glucose within the liver³⁰. Starvation induced hyperglycemia in this context is a suspected survival mechanism to provide the brain with a constant supply of glucose, allowing the animal to remain alert enough to gather/hunt for more food³⁰. However, this approach is turned deleterious under non starvation conditions or in a calorie surplus, when additional DAGs from the diet can also trigger this mechanism³⁰.

1.3.5 Skeletal Muscle Insulin Resistance

1.3.5.1 Muscle Glycogen to Hepatic Fat

Over half a century ago, studies done on rat muscle showed that incubation with fatty acids cause insulin resistance. Since then, intramyocellular lipid content has been identified as the strongest predictor of muscle insulin resistance in all populations, from children to the elderly³¹. Further ³¹P and ¹³C NMR studies revealed that it is a lipid mediated decrease in glucose transporter type 4 (GLUT4) presentation at the cell surface that limits glucose transport and is responsible for impaired insulin-stimulated muscle glycogen synthesis in T2DM^{32,33}. This occurs when an imbalance between FA delivery to the muscle cell, relative to intracellular FA oxidation or storage as neutral lipid species such as TAGs, leads to accumulation of DAGs; the molecular trigger that halts insulin receptor activation of PI3K, which is a required step for GLUT4 presentation at the cell surface and insulin stimulated glucose transport.³⁰ Binding to the insulin receptor in muscle helps mediate the uptake of circulating blood glucose by presenting more GLUT4 proteins on the cell membrane, causing efficient uptake and glycogen storage. The overall effect being decreased concentration of glucose in the blood. Mice that lack GLUT4 protein develop NAFLD quickly³⁴. Lipid-mediated muscle insulin resistance occurs when there is an increased deliverance of fatty acids to the muscle with decreased rate of mitochondrial β -oxidation^{35,36}. The resulting increase in intracellular DAG content activates the muscle isoform of PKC (PKC θ), which inhibits the insulin receptor signaling cascade, and ultimately stops the GLUT4 exocytosis and presentation on the membrane³⁶. As glucose is prevented from entering the muscle, it is shunted back to the liver where it can activate the carbohydrate response element-binding protein (ChREBP)³⁷. ChREBP, a transcription factor, causes expression of glycolytic enzymes and provides the precursors for *de novo* lipogenesis³⁷. This provides an indirect link between peripheral tissue insulin resistance and deposition of fat seen in NAFLD, by changing the fate of ingested carbohydrates from muscle glycogen to hepatic fat³⁵.

1.3.5.2 Exercise restores proper carbohydrate metabolism in muscle

Interestingly, it was found that this abnormal pattern of carbohydrate storage in insulin resistant individual was reversible with a single bout (45 minutes) of leg exercise³⁸. Insulin resistant individuals given a meal high in carbohydrates were able to restore two times their muscle glycogen content and decreased rates of DNL in their livers after exercise³⁸. Compared to liver and adipose, skeletal muscle is more sensitive to insulin and often precedes these tissues in developing insulin resistance^{35,39}. Therefore, exercise, may be the most effective way to halt T2DM, and its indirect effects on liver fat, in its tracks.

1.3.6 Adipose Tissue Insulin Resistance

1.3.6.1 Lipolysis

Adipose tissue acts as a caloric reservoir and endocrine organ that maintains systemic energy homeostasis¹⁸. In fed conditions, white adipose tissue stores glucose as fat while circulating insulin suppresses lipolysis¹⁸. Suppression of lipolysis by insulin in adipose tissue is thought to also have major effects on reducing hepatic glucose production by limiting free fatty acid flux to the liver, resulting in lowered hepatic acetyl-CoA levels through increased mitochondrial fatty acid β -oxidation and decreased pyruvate carboxylase (PC) activity¹⁸. PC is the first enzyme in gluconeogenesis. When energy is low, insulin relieves its inhibition of lipolysis, and adipose tissue supplies glycerol and free fatty acids (FFAs) to the liver, who can feed into the gluconeogenic pathway and be stored in lipid droplets, respectively¹⁸. During insulin resistance, insulin is unable to suppress lipolysis in adipose tissue, causing sustained delivery of lipid metabolites to the other organs, increasing gluconeogenesis and the prevalence of DAGs¹⁸. As previously described, ectopic fat deposition in liver and muscle will also cause insulin resistance through their own distinct mechanisms.

Additionally, FFAs contribute to other signaling pathways in the hepatocytes that trigger intrinsic apoptosis through c-Jun N-terminal kinase (JNK). Cell death in this context is thought to also promote NAFLD disease progression to NASH and cirrhosis.⁴⁰

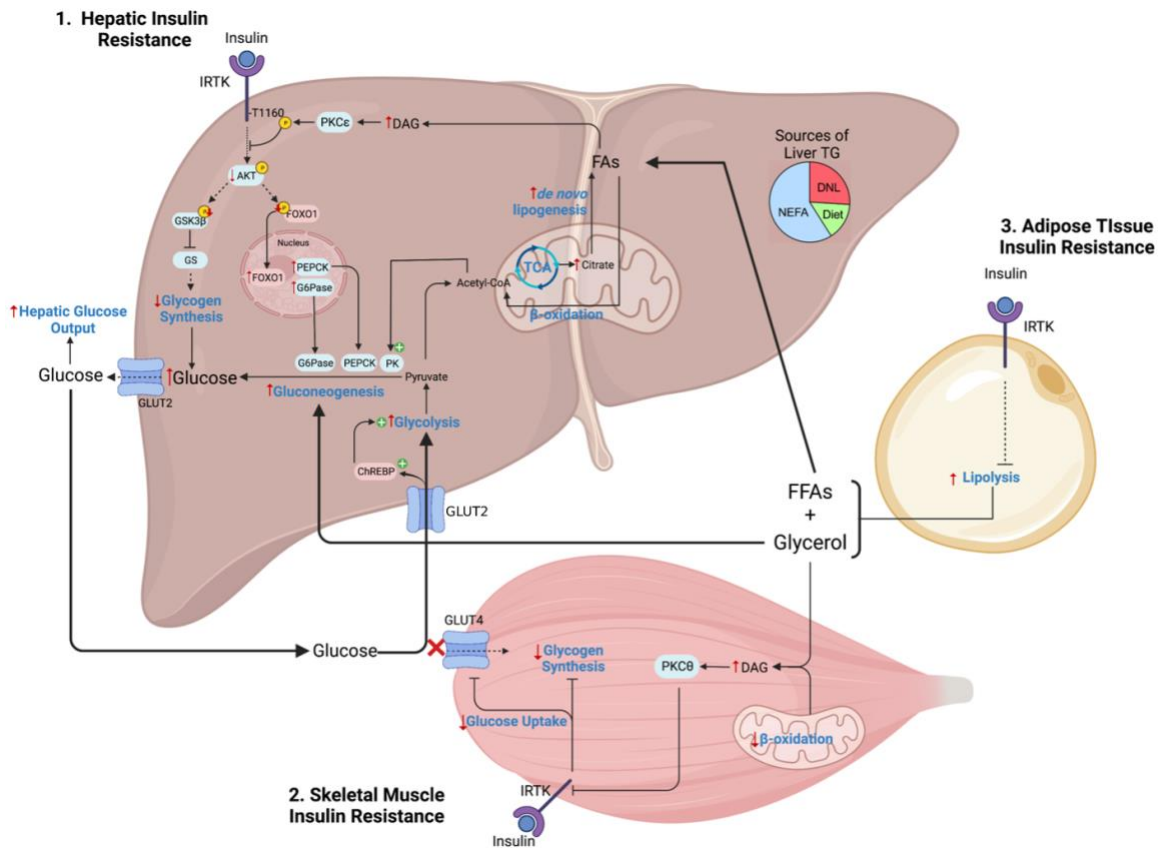


Figure C: Insulin Resistance manifests due to cross talk between liver, skeletal muscle and adipose tissue. (1) Hepatic insulin resistance manifests as decreased glycogen synthesis due to GS activity and increased gluconeogenesis due to increased FOXO1 dependant expression of PEPCK and G6Pase, ultimately resulting in increased hepatic glucose output. This occurs due to increased intracellular DAG content which activates PKC ϵ to phosphorylate inhibitory T1160 residue on IRTK, causing decreased activation of AKT. (2) Skeletal muscle insulin resistance is also driven by DAG and intramyocellular lipid content, which results in decreased glycogen synthesis and decreased GLUT4 presentation on the cell membrane. As such, glucose is shunted back to the liver where it transcriptionally activates ChREBP to activate glycolysis and DNL pathways, further driving insulin resistance in the liver. (3) Adipose tissue insulin resistance manifests as an unrepressed lipolysis, which inappropriately “spills” FFAs and glycerol to the muscle and liver. Image was produced using Biorender.

1.3.6.2 Ectopic Fat Distribution and Quantity

Large scale epidemiological studies have found that, as the body mass index (BMI) and waist circumference increase, the risk for NAFLD does as well⁴¹. Patients

with NAFLD almost universally exhibit hepatic insulin resistance⁴². It seems intuitive then, that the “dose” of ectopic body fat will push for insulin resistance⁴¹. However, there are counterintuitive cases where lack of ectopic fat can also lead to insulin resistance. Lipodystrophy is a condition characterized by fat loss in certain areas of the body, while presenting with excessive amounts of fat in the liver and muscle^{43,44}. This condition is thought to be attributable to the adipose tissue’s inability to synthesize or store TGs from the diet, instead inappropriately diverting them to the liver and muscle, causing insulin resistance^{43,44}. Fat transfers from healthy mice to lipodystrophic mice completely normalize insulin resistance and human patients can also be treated with a key missing secreted adipokine, leptin^{43,44}. In both cases, liver and muscle fat content decreased significantly, along with the concurrent disappearance of insulin resistance^{43,44}. Distribution of fat is also an important determinant of insulin sensitivity⁴⁵. In lean individuals, distribution of fat in the chest and abdominal areas as opposed to the peripheral areas have higher associations with insulin resistance⁴⁵. Lastly, prior studies by Petersen et al show that even modest weight loss (-10% of total weight) through dietary intervention sufficiently improves full body glucose metabolism, and normalized hepatic insulin sensitivity and steatosis in patients with T2DM⁴⁶. However, not all studies indicate weight loss improves NAFLD. Ultimately, it is not always the quantity of fat in the body that causes insulin resistance, but rather how the fat is distributed.

1.4 Lifestyle Management to Improve NAFLD and T2DM

The extensive cross talk between the three main insulin sensitive organs may explain the associations between T2DM and NAFLD¹⁸. Because NAFLD usually (but not always) precedes the appearance of T2DM, most treatment modalities for T2DM work surprisingly well to alleviate NAFLD¹⁸. There are several, but the three most prominent classes of drugs are hypoglycemic agents, insulin sensitizers and incretin-based therapies, with more novel drugs such as mitochondrial uncoupler agents being explored currently¹⁸. Despite secondary T2DM treatment alleviating NAFLD symptoms, there is currently no FDA approved medications for NAFLD or NASH alone⁴⁷.

Recommended cornerstone treatment for NAFLD alleviation include lifestyle alterations through increased exercise and diet modifications to modestly reduce weight⁴⁷.

2) Glucose and Fructose Metabolism

2.1 Epidemiological Trends in Sugar Consumptions

In 1977, a major shift occurred in the Western Diet⁴⁸. An ostensibly well-meaning 'Dietary Goal' was issued by the U.S. Senate that called for a reduction of saturated fat in the diet, in order to limit heart disease⁴⁸. Eager to comply, the food industry, quickly started pushing "Low-Fat" products to placate the public's worries about fat content in the diet⁴⁹. However, in order to make these new foods palatable, dietary sugar was swapped in lieu of fat^{49,50}. By 2000, 32% of total calories consumed in a Western Diet were composed of sugar⁵⁰. A comparative retrospective study done by Barlow et al. spanning from 1985-2000 also found that the impact of lowering tariffs on HFCS post-NAFTA were associated with a 41.6kcal/capita daily increase in caloric sweetener supply in Canadians⁵¹. Through increased societal exposure to added sugars, the association between US food regulation changes and the comparatively high rates of metabolic diseases seen in Canada, is concerning⁵¹. In the past 40 years, this US dietary paradigm has led to increased added sugar intake and associated with paralleled increased prevalence of obesity, diabetes and NAFLD in Canadians⁵¹⁻⁵³.

The two most common added sugars used to sweeten foods and beverages are sucrose and HFCS⁵⁴. "Added sugars" differ from "naturally occurring sugars", in that these are added during processing or preparation. This can range from a company deciding to sweeten an "organic" yogurt product to make it more palatable, to adding extra sugar to your coffee in the morning⁵⁴. This differs from naturally occurring sugars, like those present in fruits, milk, honey and sugar beets, which makes up only about 5% of the Western Diet⁵⁵. In contrast added sugar makes up three times this amount in our diets, with 42% being present in sugar sweetened beverages (SSBs) and the rest in solid foods⁵⁶. There is evidence that added sugar is more deleterious if taken in liquid form, in that participants in a study gained more weight after four weeks of consuming sucrose beverages compared to sucrose jelly beans, seemingly because it can be more

rapidly absorbed in the intestine⁵⁷. Solid versus liquid sugar diets have been minimally explored in the context of other diseases such as T2DM, NAFLD or cardiovascular diseases⁵⁵. However, comparisons of the two sugar monomers, fructose and glucose, that compose HFCS and sucrose have been extensively studied and is an area of much speculation in the field of nutrition and the popular press.

2.2 Divergent Fructose and Glucose Metabolism

Although both sugars are six membered carbon rings ($C_6H_{12}O_6$) that have an isocaloric value of 3.9kcal/g, glucose and fructose have vastly different metabolic fates in the body⁵⁸. Taskinen et al, demonstrated that only a moderate amount (300 cal per day) of excess fructose was sufficient to increase body weight, liver fat, and DNL⁵⁹. However, this study and many others like it, utilize overfeeding or *ad libitum* methods, making it impossible to separate the effects of a positive energy balance from any unique metabolic dysregulation caused by fructose. A pivotal study done by Stanhope et al, employed an energy balanced protocol to study either isocaloric glucose or fructose sweetened beverages that constituted 25% of the basal energy requirement in overweight and obese adults for ten weeks⁶⁰. Both glucose and fructose induced a similar amount of weight gain, but fructose uniquely increased DNL, insulin resistance, atherogenic dyslipidemia and visceral adiposity⁶⁰. This study challenges the “calorie in = calorie out” myth and clearly demonstrates the divergent metabolic effects fructose has from glucose, independent of positive energy consumption.

The deleterious metabolic effects of fructose seem to be magnified in sedentary people but are actually advantageous when supplied during exercise⁶¹. This is further corroborated by inspecting modern day hunter-gatherer dietary habits, such as those seen in the Tanzanian Hadza tribe⁶². Approximately 8-16% of their dietary intake is honey which mimics similar sugar intake seen in the West⁶². Despite their high fructose consumption, physical activity could mitigate the negative effects, protecting them from cardiovascular risk factors⁶².

2.2.1 Organismal Level: Gut-Liver Axis

2.2.1.1 Sugar Transporters GLUT5 and SGLT1

Upon ingestion, a high carbohydrate meal will be broken down into simple sugars (glucose and fructose) in the stomach then enter the small intestine where they can be absorbed by their respective transporters on apical poles of the enterocytes located in the brush border⁵⁸. Glucose absorption is mediated by the sodium-linked cotransporter 1 (SGLT1), which actively pumps sodium ions and glucose molecules into the cell, regardless of the concentration gradient⁶³. Fructose absorption, however, is coordinated by a facilitative transporter, GLUT5, which is most highly expressed in the proximal duodenum⁶⁴. Although this transporter has high specificity for fructose ($K_m = 6 \text{ mM}$ to 15 mM), it is sensitive to concentration gradients present across the enterocytes luminal membrane⁶⁴. The difference in the mode of action of these two transporters result in uneven dissipation of the monomers along the GI tract⁶⁵. While glucose is rapidly and almost completely absorbed in the small intestine, fructose transport capacity across enterocytes in this area can quickly be overwhelmed, leading to escape into the large intestine and fermentation by gut microbiota⁶⁵.

2.2.1.2 Absorption throughout the GI tract

Once inside the cell, a large portion of fructose will robustly be phosphorylated by ketohexokinase (KHK) into fructose-1-phosphate (F1P), which is thought to reduce the concentration gradient and aid in complete fructose absorption⁵⁸. A recent study utilizing sophisticated dual tracer approach in humans found that upon ingesting a 30 g glucose/30 g fructose drink, 85% of the fructose was metabolized by first pass gut metabolism⁶⁶. The enterocyte has the full complement of gluconeogenic enzymes and metabolizes fructose mainly into glucose, lactate, glycerate, and other organic acids⁶⁷⁻⁶⁹. Fructose metabolites and low levels of “escaped” fructose then travel through the hepatic portal vein, at a concentration of approximately 1 mM , to the liver^{70,71}. Additional fructose is extracted from the blood by hepatocytes is phosphorylated again by KHK

and used for gluconeogenesis, lipogenesis, glycogen synthesis and other metabolic pathways⁵⁸.

2.2.1.3 Circulating Levels of Fructose and Glucose

Peripheral blood exiting the liver has a negligible concentration of fructose as compared to glucose after bolus loading; 1 mM and 7.5 mM respectively in healthy individuals⁶⁶. This is reduced back down to a micromolar range upon fasting⁶⁶. Although both organs, liver and gut, are efficient at extracting fructose from the blood, the marked differences in circulating levels of the two monosaccharides is due in large part to intestinal grunt work, which shields the liver from the majority of the deleterious metabolism of fructose^{69,72}. This illustrates an additional key difference between the two sugars, in that the glucose monomer can be up taken and metabolized by all cells in the body, while fructose metabolism is constricted to mainly the gut and liver^{69,72}.

2.2.2 Cellular Fructolysis vs Glycolysis in Hepatocytes

2.2.2.1 Hexokinases KHK and GCK

Upon entrance of the hepatocyte, fructose will be cleaved into 3 carbon metabolites and added to the pools of triose-phosphates generated by other metabolic avenues like glycolysis/gluconeogenesis, lipogenesis or oxidative pathways.⁵⁸ The first of three “fructolytic” enzymes, KHK, works extremely quickly on its substrate. In fact, its capacity to phosphorylate is 10 times higher than glucose’s initial kinase, glucokinase (GCK)⁷³. This reaction is so robust that upon fructose intravenous infusions, hepatic ATP levels decline by more than 80% within minutes⁷⁴. Corresponding F1P levels measured by non-invasive ³¹P magnetic resonance spectroscopy increase 7 fold, with a quick return to basal levels after half an hour⁷⁴. Unlike KHK, GCK’s activity is tied to the energy status of the cell and is not constitutively active⁷⁵. When energy is high, glucokinase regulatory protein (GCKR) binds GCK and sequesters it from the nucleus, preventing glucose-6-phosphate (G6P) production⁷⁵. GCKR-GCK complex is stabilized

by glycolytic intermediate fructose-6-phosphate (F6P). There is no such analogous inhibitory complex seen for KHK⁷⁵.

2.2.2.2 Fructose metabolite F1P as signaling molecule

F1P presents as an interesting metabolite that can transect into hepatic glucose uptake as well⁷⁶. Catalytic quantities of F1P have been shown to disrupt the GCKR-GCK complex, allowing for GCK to translocate into the cytosol and promote glucose phosphorylation and retention⁷⁷. Thus fructose uptake into a hepatocyte facilitates glucose uptake as well⁷⁶. Fructose derived F1P produced in the gut has also been shown to elongate intestinal villus, allowing for increased absorptive capacity and energy harvest⁷⁸.

2.2.2.3 Convergence below PFK

The second fructolytic enzyme, aldolase B (ALDOB), cleaves F1P into dihydroxyacetone phosphate (DHAP) and glyceraldehyde⁵⁸. Glyceraldehyde is phosphorylated by the final enzyme in fructolysis, triokinase and FMN Cyclase (TKFC), into glyceraldehyde-3-phosphate (G3P)⁵⁸. Both of these metabolites, DHAP and G3P, can enter the glycolytic pathway downstream of its rate limiting enzyme, phosphofructokinase (PFK)⁵⁸. PFK represents the first committed step in glycolysis and is critical in the overall production and consumption of ATP⁵⁸. When glucose is absorbed into the cell it will increase glycolytic flux, which will produce both ATP and citrate, two allosteric inhibitors of PFK⁵⁸. Since fructose metabolites, DHAP and G3P, feed into glycolysis downstream of PFK, the subsequent ATP and citrate produced during TCA cycle and OXPHOS this negative feedback loop is abolished⁵⁸.

2.3 Fructose Metabolism in NAFLD and T2DM

2.3.1 Increased De Novo Lipogenesis

As mentioned above, NAFLD is characterized by intrahepatic lipid accumulation,

a condition called steatosis¹⁸. Steatosis occurs when the rate of fatty acid deposition (diet or lipolysis derived fatty acid uptake from plasma and DNL) supersedes the rate of clearance (secretion through very-low-density lipoproteins and fatty acid oxidation (FAO))²⁵. Tracer experiments done in NAFLD patients estimate that only 26% of intrahepatic lipid content is derived from DNL, whilst 59% and 15% are designated to circulating FAs and dietary fat, respectively⁷⁹. However, when compared to matched controls lacking any fatty liver phenotype, these subjects had similar circulating FAs and dietary fat derived intrahepatic content, but had a 3 fold decrease in DNL⁷⁹. This suggests that DNL is a distinct pathological pathway driving NAFLD^{79,80}.

Fructose metabolism can contribute to increases in hepatic DNL in multiple ways. Firstly, as discussed above, fructose and glucose metabolic pathways converge after the production of triose phosphate intermediates DHAP and G3P⁵⁸. By bypassing PFK fructose uniquely induces unregulated glycolytic and TCA flux, causing citrate to be shuttled into the cytosol, cleaved by ATP citrate lyase (AclY) to generate acetyl-CoA; the preliminary substrate for DNL⁵⁸. However, fermentation of stray fructose molecules by gut bacteria, can also produce acetate extra-hepatically⁶⁵. Following transport through the portal vein, microbiota-derived acetate can be catalyzed by acetyl-CoA by an acetyl-CoA synthetase (Acss2) into acetyl-CoA as well. These metabolic pathways provide both a direct and indirect mechanism for fructose derived substrates to contribute to DNL⁶⁵.

2.3.2. Transcriptional Regulation: ChREBP and SREBP-1c

The major mechanism by which fructose drives NAFLD is through the metabolite F1P which releases GCK from its inhibitor binding partner GCKR⁷⁵. The subsequent upregulation of triose phosphates stimulates carbohydrate sensing transcription factor ChREBP⁸¹. Within the liver, ChREBP induces key glycolytic and lipogenic enzymes and transactivates all three fructolytic enzymes as well^{82,83}. Fructose feeding quickly induces the highly active isoform ChREBP_a in diabetic, steatotic and obese human livers^{84,85}. Liver specific knockdowns of ChREBP prevents fructose mediated induction of DNL genes, *ACC2*, *FAS*, *SCD1* during excessive fructose diets. However there were no improvements in hepatic steatosis or insulin sensitivity as compare to controls;

suggested to be due to an equal decreased expression of VLDL packaging export proteins like MTP⁸⁶⁻⁸⁸. The rate of VLDL secretion in a normal liver is 11.4 ± 1.1 $\mu\text{mol}/\text{min}$, while this increases two-fold in human subjects with NAFLD at 24.3 ± 3.1 $\mu\text{mol}/\text{min}$.⁸⁹

Nutrient and hormone sensitive transcription factor, sterol regulatory element binding protein-1c (SREBP1-c), works synergistically with CHREBP to activate lipogenic enzymes⁸⁸. Insulin signaling causes increased mRNA synthesis and processed nuclear forms of SREBP-1c through an AKT/mTORC1/lipin-1 mediated phosphorylation cascade⁹⁰. Although fructose cannot directly stimulate pancreatic beta-cells to secrete insulin⁹¹, the associated adiposity and resulting hyperinsulinemia secondary to high fructose feeding causes indirect activation of SREBP-1c.

2.3.3. Decreased Fatty Acid Oxidation

In addition to acting as raw substrate for DNL, fructose metabolites also transcriptionally regulate this pathway through CHREBP and SREBP1-c in the liver. There is recent evidence that fructose not only promotes DNL in the liver, but also prevents FAO⁹². Acetylation of key mitochondrial proteins involved in FAO, acyl-CoA dehydrogenase long chain (ACADL) and carnitine palmitoyltransferase-1a (CPT-1a), as well as decreased FAO enzyme expression occurs in livers of mice on a 10-week high fructose/ high fat diet⁹². These results were not seen in an isocaloric high glucose/ high fat diet, cementing that fructose is a uniquely deleterious sugar to be coupling with high fat meals, as it not only promotes fat accumulation but prevents fat burning as well⁹².

3. Nuclear Receptors

3.1 Transcriptional Regulation of Energy Homeostasis

The concept of the “interior milieu” was first defined by physiologist Claude Bernard as the body’s ability to keenly monitor its internal conditions and adapt if any perturbations were to compromise stability. This is true on an organismal and organ level, for example during exercise the heart will increase blood flow to meet the body’s

increased metabolic demands, but also can occur at the cellular level as well⁹³. After the body's fuel requirements for its basal metabolic rate is met, different cell types are responsible for a balanced regulation of fuel intake, storage and expenditure in response to developmental and physiological needs⁹³. Short term adaptation is accomplished by hormones which trigger complex biochemical pathways in metabolically active organs⁹³. For example, in acute phase exercise, testosterone, HGH and IGF are produced to repair damaged tissue. Long term exercise will cause an increased presentation of corresponding receptors on the surface of myocytes, allowing for more effective repair. But in this instance, what maintains this sustained presentation on the surface of the cell? Transcriptional control of metabolic genes is the answer to long term adaptation to a specific physiological stimulus⁹³. Nuclear receptors are a class of transcription factors that, in response to a chemical ligand, like vitamins, metabolites, small lipophilic hormones or drugs, will act in the nucleus to regulate gene expression⁹³. Loss or gain of activity of these proteins have been extensively implicated in the aetiology of a variety of metabolic related diseases such as obesity, T2DM, NAFLD and cancer⁹³.

3.2 The Estrogen Related Receptors

Of the 48 nuclear receptors encoded in the human genome, a subgroup termed the "orphan nuclear receptors" lack an identified endogenous ligand to modulate their activity⁹⁴. Instead, they rely on a host of co-activator and co-repressor proteins to modulate their activity as transcription factors⁹⁴. The estrogen related receptor (ERRs) subfamily were the first orphan nuclear receptors to be identified and hold a central role in energy metabolism⁹⁴. Three members, ERR α , ERR β and ERR γ , work to integrate long term or adaptive responses to carbohydrate, lipid and mitochondrial metabolism⁹⁴. The first two, ERR α and ERR β , were discovered during a screen to identify steroid hormones receptors similar to the estrogen receptor- α (ER α) within the kidney and heart, whilst the third, ERR γ was identified a decade later^{95,96}. Compared to ERR β and γ , ERR α expression throughout the body is more abundant, with particular hotspots

located in metabolically active tissues such as the liver, skeletal muscle, brown adipose tissue, intestine, kidney and heart^{93,97}.

3.3 Structure of the ERRs

3.3.1 Amino Terminal Domain

The ERRs represent the canonical orphan nuclear receptor, which has three characteristic structural features (Fig. D)⁹⁸. The first is a NTD, that contains sites for post translational modifications such as phosphorylation and sumoylation to modulate their activity. For example, phosphorylation sites exist at serine residues 19 and 22 of ERR α , and a S19A mutation has been shown to increase the transcriptional activities of ERR α in the presence of co-regulators^{99,100}. In fact, S19 and S22 in ERR α are also major phosphorylation sites in breast cancer cells^{99,100}. This finding was further expanded in 2022 by Hui et al, in that a three consensus phosphorylation motif for the kinase GSK3 β were elucidated through bioinformatic analysis⁹⁴. Serines 19, 22 and 26 with an additional “priming” glutamic acid residue at position 30 were found to be insulin stimulated phosphorylation sites responsible for protecting ERR α against degradation⁹⁴. In the absence of insulin signaling GSK3 β is activated and phosphorylates these sites, priming them for ubiquitination and subsequent proteasome degradation⁹⁴. Sumoylation of both ERR α and ERR γ is also possible in the NTD, as it contains a functional phospho-sumoyl switch motif $\Psi KxEPxSP$ ¹⁰¹. This is thought to play a role in regulating interactions between transcription factors that form higher order structures¹⁰¹. The ERR NTD is dissimilar from other types of nuclear receptors but remains well conserved between the three members, suggesting it is crucial for their specialized function^{99,100}.

3.3.2 DNA Binding Domain

To regulate transcription, nuclear receptors are required to recognize key short DNA sequences distributed throughout the genome. These consensus sequences are termed the ERR response elements (ERRE) for the ERR subfamily and are located

either at promoter sites or distal from the transcriptional start site of a gene⁹³. The ERRE, defined as TCAAGGTCA was identified using a selection and amplified binding (SAAB) technique in 1997 by Sladek et al. and was later confirmed by ChIP-seq analysis¹⁰². All three ERRs are capable of binding to ERRE's throughout the genome, therefore, most target genes harboring an ERRE can be potentially regulated by all three ERR isoforms¹⁰³. The ERR isoforms can bind DNA as a monomer or as homodimer or heterodimer complexes¹⁰³⁻¹⁰⁶. The ability of the ERRs to bind to the ERRE is dynamically affected by acetyltransferase p300 coactivator associated factor (PCAF) and deacetylases such as HDAC8 and sirtuin 1 homolog (SIRT1), which post translationally modify four conserved lysine residues in the DBD, changing the state of chromatin structure¹⁰⁷.

3.3.3 Ligand Binding Domain

The ligand binding domain (LBD) contains a well conserved activation function-2 (AF-2) motif^{108,109}. In nuclear receptors that are capable of binding substrate, the AF-2 domain moves into an 'active' state once a small lipophilic encounter the binding pocket^{108,109}. However, crystal structures of ERR α and ERR γ have revealed that their AF-2 domain is in constitutively active configuration^{108,109}. Although an orphan nuclear receptor, regulation of ERRs' activity is dependent on their co-regulator's affinity for binding and their relative concentration within a tissue, as well as binding of synthetic drugs using the well-defined LBD pocket shown by crystallographic studies¹⁰⁸.

3.4 ERR α Regulation

As mentioned, the activities of orphan nuclear receptors in the absence of any natural ligand fall to a group of more than 200 co-regulator proteins: each one displaying differential expression patterns, enzymatic activity, or specificity⁹⁴. The majority of studies published on the ERRs surround ERR α , as such it will be the focus of this introduction.

3.4.1 Co-Activator PGC-1 α

One of the most notable and potent coactivators of the ERRs are members of the PGC-1 family. Broadly, the PGC-1 α coactivators act as direct sensors of metabolic needs and fine tune the activity of multiple nuclear receptors¹¹⁰. PGC-1 α itself is directly regulated by energy sensing complexes such as AMPK (sensitive to AMP), SIRT1 (sensitive to NAD⁺) and GCN5 (histone acetyltransferase)^{111,112}. In particular, AMPK monitors the ratio of AMP to ATP within the cell, and once activated will begin to phosphorylate substrates to decrease ATP consumption and increase ATP generation, promoting an overall catabolic state¹¹¹. It can indirectly modulate the activity of nuclear receptors by phosphorylating PGC-1 α . PGC-1 α occupies a central role in energy homeostasis as it is implicated in mitochondrial biogenesis, oxidative phosphorylation (OXPHOS), fatty acid oxidation, (FAO), adaptive thermogenesis, glucose uptake, glycolysis, hepatic gluconeogenesis, ketogenesis, and circadian activity¹¹⁰. In particular PGC-1 α and ERR α display similar expression patterns in metabolically active organs and act together to regulate various metabolic events^{102,113,114}. ERR α can drive the expression of *Pargc1a* by binding to a distal enhancer site, which then works in an auto-regulatory feedforward loop to intensify the activity of ERR α by acting as a binding partner¹¹⁵. This complex was first identified in yeast two-hybrid screen of a cardiac cDNA library¹¹⁶. Additionally, LXXLL motif at position 142-146 within PGC-1 α is necessary for binding other nuclear receptors^{116,117}. However, the identification of an additional leucine rich motif at positions 209-213 within PGC-1 α cemented a unique interface in which only the three ERR isoforms could interact with^{116,117}. Activation of AMPK causes increased PGC-1 α /ERR α complex expression and binding of cognate ERR α sites and overall increased mitochondrial biogenesis and increased energy reserves^{112,118}. However, in breast cancer cells, the PGC-1 α /ERR α complex renders breast cancer cells susceptible to anti folate therapy by downregulating genes involved in 1C metabolism¹¹⁹. However, AMPK activation of the PGC-1 α /ERR α complex has also been associated with adipose tissue browning, due to transcriptional increase in mitochondrial function, lipid oxidation and energy expenditure¹¹⁸.

3.4.2 Co-Repressors NCoR1, PROX1 and NRIP

On the other hand, the transcriptional activity of $ERR\alpha$ can be repressed by the ubiquitously expressed corepressor, NR corepressor 1 (NCoR1)¹²⁰. NCoR1 functions by forming a “locked” chromatin state through recruitment of histone deacetylase 3 (HDAC3)¹²⁰. In global gene expression studies in muscle, the effect of NCoR1 deletion on the expression on metabolic genes is highly analogous to PGC-1 α overexpression^{121,122}. The binary action between PGC-1 α and NCoR1 is thought to be due to the use of a common binding pocket, conferring clear opposing effects on $ERR\alpha$ activities¹²³. The current working model suggests that because NCoR1 is expressed at basal levels, it will occupy $ERR\alpha$ until some external stimuli, like cold exposure or exercise, prompts an exchange with a coactivator like PGC-1 α ¹²¹. Mice with total or liver specific knockouts for NCoR1 display several metabolic dysfunctions including glucose intolerance, insulin resistance, adipose-associated inflammation and reduced respiration potential¹²¹. It has also been shown to be phosphorylated in response to insulin stimulation, causing simultaneous depression of Liver X receptor alpha (LXR α) to drive energy storage and lipogenesis while inhibiting $ERR\alpha$ and PPAR α to prevent oxidative metabolism or energy production¹²⁴. PROX1, the prototypical and highly conserved nuclear receptor corepressor, was also found to be a negative modulator of the $ERR\alpha$ /PGC-1 α transcriptional axis using CHIP-on-chip experiments in mouse like and bound 40% of $ERR\alpha$ target genes¹²⁵. PROX1 has been shown to be essential for the development of several metabolic organs, including the liver and its distinct hepatic cistromes overlap heavily with those of $ERR\alpha$, causing decreased expression of lipid handling and respiratory capacity programs¹²⁵. Mice with liver specific KO of this co repressor exhibit insulin resistance, while human liver with depleted expression have increased TG content¹²⁶. Lastly nuclear receptor interacting protein 140 (RIP140) has also been shown to differentially regulate $ERR\alpha$ transactivation depending on target genes¹²⁷.

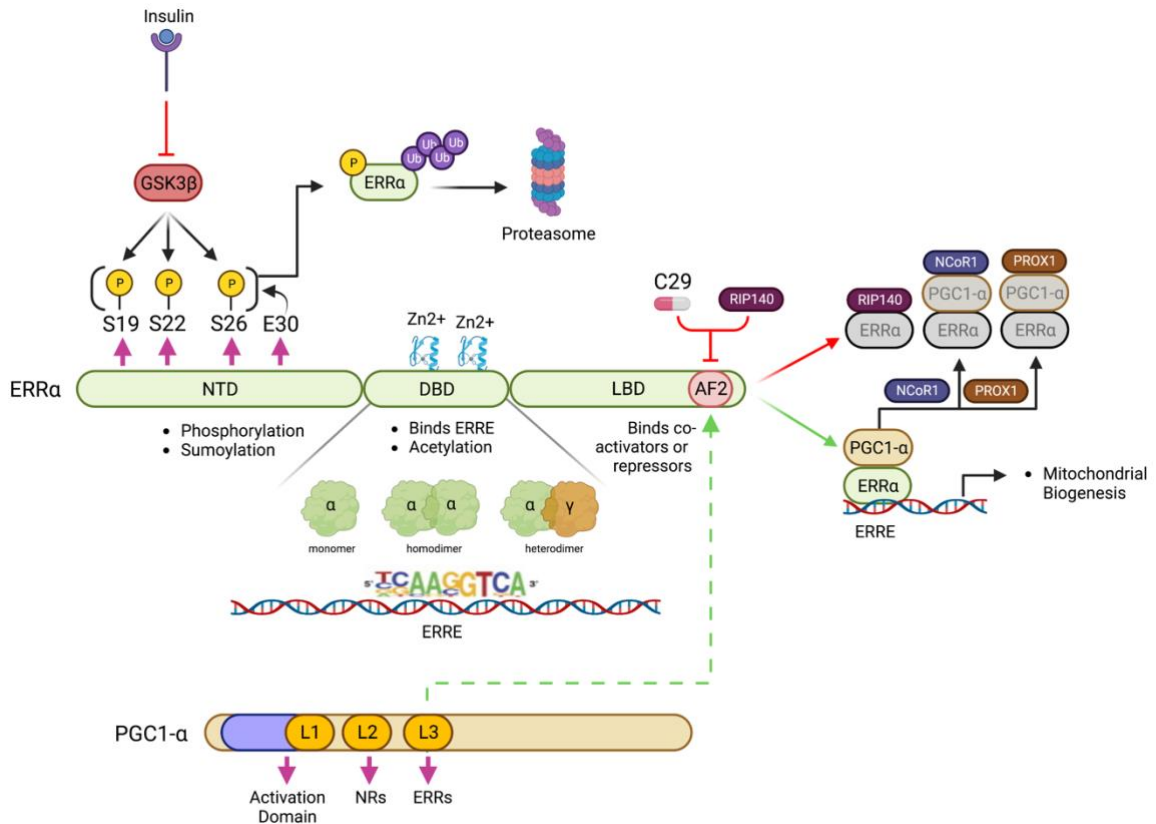


Figure D: Structure and Interactions of ERR α . ERR α is composed of three main parts. A NTD that is subject to post translational modifications such as phosphorylation and sumoylation. In particular, serine 19, 22 and 26 and a priming glutamic acid residue at position 30 are sensitive to GSK3 β induced phosphorylation, which causes ubiquitination and proteasomal degradation. The DBD contains a zinc finger that aids in binding to the ERRE, either as a monomer, homodimer or heterodimer. The LBD, binds coactivators like PGC1- α on its third leucine rich motif via the AF2 domain and corepressors like NCoR1 and RIP140. ERR α can also be inhibited pharmacologically by C29, which is an inverse agonist that also targets the LBD. Image produced in Biorender.

3.5 The Role of ERR α in Energy Metabolism

3.5.1 ERR α Transcriptomic Studies

The first target gene of ERR α to be identified was medium-chain acyl coenzyme A (*Acadm*); the enzyme catalyzing the initial step of the mitochondrial fatty acid β -oxidation pathway¹⁰². Early studies trying to identify direct ERR α target genes were slow, as it involved manual inspecting for binding sites of promoter regions. Of note, before genome wide transcriptional profiling was available, identified targeted ERR α

genes were involved in OXPHOS pathways, mitochondrial biogenesis (*mTFA*, *Tim22*, *IDH3A*, *CPT1A*, *Cyts* and *ATPsynβ*), FOA (*Acadm*), glucose utilization (*PDK4*, *Gck*), gluconeogenesis (*Pck1*), and itself (*Esrra*), just to name a few. Important to note, the ability of $ERR\alpha$ to stimulate most of these pathways were reliant on the co-activator $PGC-1\alpha$ to carry out its function in a context and tissue specific manner.

The first ChiP-on-chip study done in the heart confirmed these findings and expanded on the repertoire of direct $ERR\alpha$ targets; providing a more comprehensive view of $ERR\alpha$ function¹⁰³. ChiP-on-chip studies done in the liver, the central metabolic organ of the body, further revealed that $ERR\alpha/PGC-1\alpha$ binds clusters of functionally linked genes; the promoter of every gene involved in glycolysis, the TCA cycle and pyruvate metabolism were bound and regulated by $ERR\alpha$ ¹²⁵. This cluster of functionally linked genes, termed the $ERR\alpha$ bioenergetic regulon, is involved in the generation of energy from glucose and is negatively regulated by a trimeric complex consisting of $ERR\alpha$, $PGC-1\alpha$ and $PROX1$ ¹²⁵. Further characterizations of $ERR\alpha$'s transcriptional gene networks were identified by subsequent ChiP-seq experiments in the liver, which corroborated previous findings that $ERR\alpha$ also regulates mitochondrial function and DNL¹²⁸.

3.5.2 Phenotype of the $ERR\alpha$ mouse models

Further proof that $ERR\alpha$ was involved in lipid metabolism came from in vivo experiments using the $ERR\alpha$ null model (Fig. E)¹²⁹. The $ERR\alpha^{-/-}$ mice were observed to be lean, resistant to high-fat diet induced obesity and displayed increased insulin sensitivity and hypoglycaemia with “red” livers (indicating no steatosis)¹²⁹. These mice also cannot survive cold exposure either^{130,131}. Additionally, the circadian dependant expression of $ERR\alpha$ is achieved by a transcriptional regulatory loop with $BMAL1$, and $ERR\alpha$ KO mice exhibit dysfunctional locomotor activity, abnormal circadian rhythm and altered circulating diurnal lipid profiles¹³². Pharmacological inhibition of $ERR\alpha$ through administration of compound 29 (C29), a highly selective inverse agonist, in diabetic or obese mice also improved insulin sensitivity by reducing circulation glucose, FFAs and TGs¹³³⁻¹³⁵. During trials of fasting and refeeding, robust repression of

hepatic DNL gene expression during a HFD was due to the absence of $ERR\alpha$ in KO mouse models and prevented steatosis and NAFLD-like symptoms in mice¹³⁶. Conversely $ERR\alpha$ was necessary for post prandial hepatic TG clearance and alleviation of NAFLD in these mice¹³⁶. The role of $ERR\alpha$ is also relevant in pharmacologically-induced NAFLD, in that its absence aggravates the progression of rapamycin induced NAFLD livers¹²⁸. Rapamycin is used as an immunosuppressant to improve allograft success rates and is an acute inhibitor of mTORC1¹²⁸. $ERR\alpha$ and nuclear mTOR mouse liver CHIP-seq findings described by Chaveroux et al. showed that, although $ERR\alpha$ and mTOR do not interact physically on DNA, they do regulate 3667 common genes; genes that are involved in OXPHOS, the TCA cycle, glycolysis/gluconeogenesis, and lipid metabolism¹²⁸. mTOR activity was found to be protective against ubiquitination and subsequent proteasome mediated degradation of $ERR\alpha$ ¹²⁸. Concurrent loss of mTOR activity via rapamycin treatment and $ERR\alpha$ absence in KO mice resulted in acute dysregulation of the above mentioned pathways and aggravated NAFLD as compared to WT mice¹²⁸. As such it is intuitive that mTOR inactivity signals low energy and a cessation of anabolic pathways, therefore degrading $ERR\alpha$ and halting its energy producing gene programs¹²⁸. It is thought that the beneficial ablation of whole body $ERR\alpha$ is protective against HFD induced obesity, NAFLD and glucose intolerance due decreased expression of a target gene, apolipoprotein B48 which consequently prevents dietary lipid absorption in the gut. To circumvent this, the generation of a liver specific knockout of $ERR\alpha$ (LKO- $ERR\alpha$) was generated to attempt to eliminate secondary effects from the gut. Interestingly, LKO- $ERR\alpha$ mice display a divergent phenotype from whole body $ERR\alpha^{-/-}$ mice, in that a HFD exacerbated fatty liver with decreased expression of fatty acid metabolic genes coupled with insulin resistance and glucose intolerance. A small molecule agonist for $ERR\alpha$ developed by the same group, JND003, was able to provide a “proof of concept” that increased activity of this receptor could rescue this phenotype, as it re-increased the lipid and glucose catabolism genes lost in the LKO¹³⁷. For this reason, agonism of $ERR\alpha$ could present a therapeutic strategy for metabolic diseases¹³⁷.

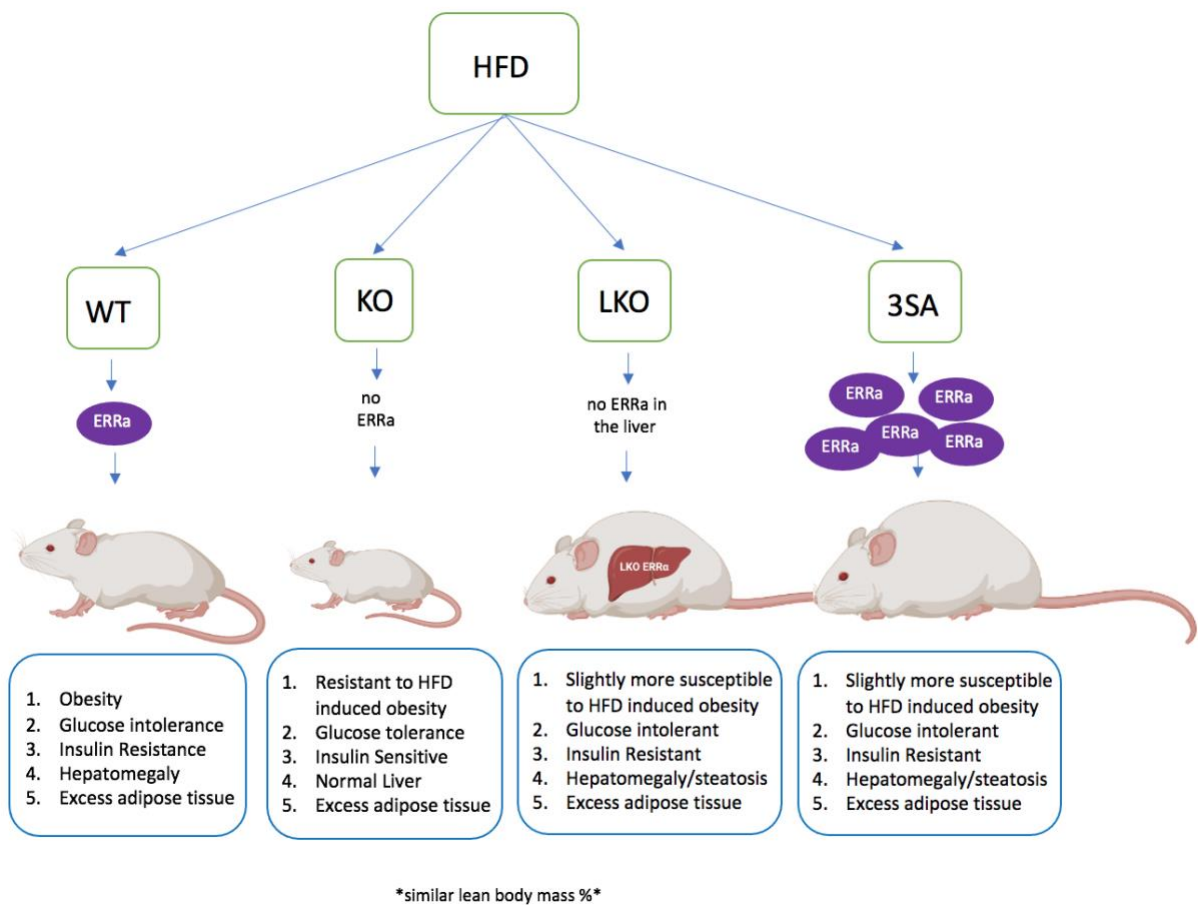


Figure E: In vivo models for $ERR\alpha$ activity. When put on a HFD Wildtype will gain weight and become obese, with accompanying glucose intolerance, insulin resistance and hepatomegaly (due to steatosis). $ERR\alpha^{-/-}$ mice however, are resistant to HFD induced obesity, remain glucose tolerant and insulin sensitive, whilst preserving the weight and health of their liver by storing excess fat only in adipose tissue. Interestingly, in the liver specific knockout of $ERR\alpha$, this phenotype is reversed, highlighting that absent lipid gut absorption contributed a large part of the protective phenotype seen in the original model. $ERR\alpha^{3SA}$ mice, with excess protein expression, have severed insulin mediated action of $ERR\alpha$, and are thus insulin resistant, glucose intolerant and are slightly more susceptible to HFD-induced obesity. Image produced in Biorender

3.6 Contributions to Metabolic Disease

3.6.1 Glucose Metabolism and Insulin Resistance

$ERR\alpha$ plays a major role in development of insulin resistance, both through transcriptional regulation of glucose handling and gluconeogenesis⁹⁴. Firstly, it regulates the presentation and expression of GLUT4, and once glucose has been phosphorylated

by GCK into G6P, it will enter the glycolytic pathway to produce pyruvate and two molecules of ATP¹³⁸. This is also regulated by ERR α , as all enzymes of the glycolytic pathway fall under the control of previously mentioned ERR α bioenergetic regulon¹²⁸. The next step, involves the conversion of pyruvate to acetyl-CoA. Under conditions of acute exercise in mice, the PGC-1 α /ERR α transcriptional axis works to up regulate the expression of *Pdk4* in skeletal muscle¹³⁹. Pyruvate is the end product of glycolysis and represents a major branching point in metabolism. This metabolite can participate in anaerobic glycolysis (lactate), the Cahill cycle (alanine), TCA cycle metabolite replenishment (Oxaloacetate) or most importantly OXPHOS (acetyl-CoA). The enzyme responsible for converting pyruvate into acetyl-coA is pyruvate dehydrogenase (PDH) and is a critical, irreversible and rate limiting step in the glucose oxidation. Post-translational control of PDH by a family of pyruvate dehydrogenase kinases (PDKs), inactivates the complex and favours FAO over OXPHOS. CHIP assays identified ERR α (and *Gabpa*) as an important mediator of PGC-1 α induced *PDK4* expression in diabetic muscle, which is in line with observations of reduced OXPHOS expression in diabetic human skeletal muscle¹⁴⁰. Further evidence to support this is that PGC-1 α activating of ERR α also induces expression of *Gck*, which improves glucose uptake, glycolytic flux, glycogen synthesis and could potentially aid in reducing hyperglycaemia⁹⁴.

Although these two proteins work together to up regulate FAO in muscle, their effect on gluconeogenesis in the liver is diametrically opposed. ERR α has been suggested to prevent the binding of PGC-1 α to the proximal region of phosphoenolpyruvate carboxykinase gene (*PEPCK*), which encodes the rate determining enzyme in gluconeogenesis^{141,142}. This has important implications on the development of hepatic insulin resistance, as it is defined by the inability of insulin to halt glucose output in the liver^{141,142}. In studies of insulin resistant humans, there is a reduction in ERR α target genes¹⁴³. In 2022, a direct link between insulin signaling and the stability of the ERR α protein was found¹⁴⁴. Three phosphorylation sites on ERR α , S19 S22 and S26, were found to be modified by GS3K β in the absence of insulin¹⁴⁴. The phosphorylation of these sites trigger ubiquitination and recruitment of the E3 ligase FBXW7 α for

proteasomal degradation of $ERR\alpha$ ¹⁴⁴. Abrogation of these sites by mutation to alanine in mice, generate a phosphorylation-mutant $ERR\alpha^{3SA}$ mouse which display an opposing phenotype observed with the $ERR\alpha^{-/-}$ mice¹⁴⁴. The $ERR\alpha^{3SA}$ mice were slightly more susceptible to HFD, had modest steatosis, and displayed glucose intolerance and insulin resistance during GTT and ITT tests¹⁴⁴. This condition was ameliorated via administration of C29 into $ERR\alpha^{3SA}$ mice on a 17-week HFD, supporting a therapeutic role for antagonizing $ERR\alpha$ activity in metabolic diseases¹⁴⁴. This highlight's $ERR\alpha$ dynamic role in metabolic regulation, as it's antagonism and agonism have both been proposed as therapeutic depending on the context (NALFD vs healthy liver, during fasting and refeeding, etc.)

3.6.2 Lactate Metabolism

When oxygen is not available, cell will switch from OXPHOS to anaerobic metabolic to convert pyruvate into lactate instead of acetyl-CoA¹⁴⁵. This fermentation reaction is catalyzed by lactate dehydrogenase (LDH) and forms two ATP molecules¹⁴⁵. This metabolism is favored in breast cancer cells, where glucose levels are extremely low (<1mM) due to rapid metabolism and uptake and suggests they can pivot to lactate as a primary source of energy to survival extended periods of glucose deprivation¹⁴⁵. Cancer cells often develop resistance towards mTOR and PI3K inhibitors for this reason¹⁴⁵. It was found that $ERR\alpha$ was able to regulate several genes involved in lactate metabolism including lactate dehydrogenase B (LDHB) and monocarboxylate transporter 1 (MCT1), and pharmacological inhibition of $ERR\alpha$ resulted in compromised lactate metabolism¹⁴⁵.

3.6.3 Lipid Utilization

Once a FA has been transported into the cell, it is covalently linked to a CoA molecule and are bound to a carnitine molecule to form an acylcarnitine in the cytosol¹⁴⁶. Carnitine binding, allows it to be targeted by carnitine palmitoyltransferase 1

(CPT1) on the outer mitochondrial membrane for translocation, subsequent rebinding to CoA and conversion into a fatty-acyl-CoA for FAO within the mitochondria¹⁴⁶. This process involves sequential ligations of the fatty acyl chain to produce molecules of acetyl-CoA¹⁴⁶. All three isoforms of ERR α and PPAR α transcriptionally regulate the genes involved in this process¹⁴⁶.

3.6.4 Mitochondrial Biogenesis, Fusion and Fission

In order to adapt to the needs of the tissue, the shape, number and distribution of mitochondria will change. Mitochondrial biogenesis is largely coordinated by transcription factor mitochondrial transcription factor A (TFAM), mitochondrial transcription factor B1 (TFB1M) and TFB2M for the generation of mtDNA and nuclear respiratory factor 1 (NRF1) and NRF2)^{103,130,140,147}. All of these are under the control of ERR α and PGC-1 α action to coordinate mitochondrial biogenesis^{143,148,149}.

Mitochondrial fusion and fission are mitigated by several proteins. For example, fission is due to the action of the GTPase dynamin-related protein 1 (DRP1) and fusion is regulated by two proteins for each layer of the mitochondrial membrane; the inner membrane is regulated by optic atrophy 1 (OPA1) and the outer by mitofusin 1 and 2 (MFN1 and MFN2)^{150,151}. MFN2 is directly regulated by ERR α/γ in muscle and heart and knockouts display decreased expression for almost all proteins required for fission and fusion^{150,151}.

3.7 ERR α as a Metabolic Transcriptional Hub

A transcriptional hub is a biochemical phenomenon by which multiple external stimuli converge onto the action of a transcription factor which bears the responsibility of integrating these signals in order to get granular genomic expression patterns¹¹⁰. As mentioned, ERR α activity is highly dependent on what PTM are added to it, the presence or absence of its co regulators and its overall rate of expression and degradation, centering it as a transcriptional hub for metabolic activity¹¹⁰. In order to qualify as a regulator of a metabolic hub, a transcription factor must be sensitive to four different things; external stimuli, internal energy state of the cell, nutrient availability and

hormonal cues¹¹⁰. To summarize the studies mentioned in this review, ERR α meets all of these criteria. First, it is able to react to external stimuli such as cold exposure and exercise with the aid of its protein ligand PGC-1 α , as well as maintaining circadian expression throughout a 24 hour cycle with BMAL1/PROX1 interactions^{114,132,152}. Secondly, ERR α is sensitive to NAD⁺ levels through Sirt1 acetylation of PGC1- α and AMP:ATP ratios through AMPK phosphorylation of PGC1- α ¹¹¹. Third, it is sensitive to available nutrients such as glucose and amino acids, as its degradation is tied to the presence of mTOR dependent repression of proteasome related genes¹²⁸. Lastly, it is sensitive to hormonal cues, as 3 phosphorylation sites in its NTD are reduced during insulin signaling cascades, saving it from degradation again.¹⁴⁴

In conclusion, our current knowledge of ERR α role as a metabolic transcriptional hub is not fully understood and it complicated by the fact that it can play both a pathological and physiological role depending on the context⁹⁴. It must be noted that other nuclear receptors also present as potential transcriptional hubs, possibly up to 48 unique ones¹¹⁰. In order to move towards potential therapeutic cures for metabolic diseases, a unified and integrated understanding of all of these hubs must be undertaken¹¹⁰. This manuscript will focus only on the individual activities of ERR α in an attempt to tackle its individual contribution to total energy homeostasis.

X. RESULTS

Sugar diet induced weight gain in ERR α mouse models

Male wildtype (WT), ERR α ^{-/-} and ERR α ^{3SA} mice were fed a low-fat diet (LFD) or a 60% HFD supplemented with water, 30% glucose or 30% fructose, starting at 6 weeks of age for 10 consecutive weeks. On a control LFD supplemented with water alone, ERR α ^{-/-} mice gained less weight on average compare to WT, while ERR α ^{3SA} gained a similar amount of weight (Fig. 1, a,b). WT, ERR α ^{-/-} and ERR α ^{3SA} mice had a similar caloric intake of 81.51, 73.57 and 81.2 kcal/mouse/week, respectively (Fig. 1, c and Table 1). On a 60% HFD supplemented with water, as expected, WT mice gained more weight than just on the LFD (Fig. 1, a,b). They also had an increased caloric intake of 104.14 kcal/mouse/week, as compared to LFD (Fig. 1, c and Table 1). As previously reported, ERR α ^{-/-} mice were resistant to HFD-induced obesity as compared to WT, although it was not statistically significant at this experimental end point (10 weeks) (Fig. 1, a,b). ERR α ^{-/-} mice had slightly less caloric intake, as compared to WT at 93.04 kcal/mouse/week (Fig. 1, c and Table 1). ERR α ^{3SA} mice were slightly more susceptible to HFD-induced obesity as compared to WT, although it was not statistically significant (Fig. 1, a,b). ERR α ^{3SA} mice had slightly less caloric intake, as compared to WT at 95.97 kcal/mouse/week (Fig. 1, c and Table 1).

On a control LFD supplemented with 30% (w/v) glucose, similar trends appear. ERR α ^{-/-} mice gained less weight on average as compared to WT, while ERR α ^{3SA} gained similar amounts of weight (Fig. 1, d,e). WT and ERR α ^{-/-} mice on this diet condition had similar caloric intakes of 95.67 and 93.04 kcal/mouse/week, respectively, while ERR α ^{3SA} mice consumed slightly more at 102.48 kcal/mouse/week (Fig. 1, f and Table 1). On a HFD supplemented with glucose, as expected, WT mice had increased weight gain as compared to LFD supplemented with glucose (Fig. 1, d,e). They also had an increased caloric intake of 106.91 kcal/mouse/week (Fig. 1, f and Table 1). ERR α ^{-/-} mice were resistant to weight gain on a HFD supplemented with glucose as compared to WT (Fig. 1, d,e). Unexpectedly, glucose supplementation in this context caused ERR α ^{-/-} mice to gain even less weight just a HFD with water, with endpoint body weights at 10

weeks averaging at 34.92 g and 38.24 g, respectively (Fig. 1 a,b and d,e). This decreased weight gain for $ERR\alpha^{-/-}$ mice on a HFD supplemented with glucose is not explained by decreased caloric intake, in fact these mice consumed 103.00 kcal/mouse/week, which is more than the mice that were just on HFD supplemented with water that consumed 93.04 kcal/mouse/week (Fig. 1 c and f and Table 1). $ERR\alpha^{3SA}$ mice gained similarly on a HFD supplemented with glucose as compared to WT (Fig. 1, d,e). They also had similar caloric intake to WT, at 105.43 kcal/mouse/week (Fig. 1, c and Table 1).

On a control LFD supplemented with 30% (w/v) fructose, $ERR\alpha^{3SA}$ mice gained less weight on average as compared to WT, while $ERR\alpha^{-/-}$ gained similar amounts of weight (Fig. 1, g,h). WT and $ERR\alpha^{-/-}$ mice on this diet condition had similar caloric intakes of 77.56 and 76.21 kcal/mouse/week, respectively, while $ERR\alpha^{3SA}$ mice consumed slightly more at 89.86 kcal/mouse/week despite decreased weight gain (Fig. 1, i and Table 1). Similar trends appear on a HFD supplemented with fructose, in that $ERR\alpha^{3SA}$ mice gained less weight than WT and $ERR\alpha^{-/-}$ (Fig. 1, g,h), despite a decreased caloric intake of 93.76 as compared to 101.05 and 106.36 kcal/week/mouse, respectively. Unexpectedly, fructose supplementation caused $ERR\alpha^{3SA}$ mice to gain even less weight than just HFD with water, with endpoint body weights at 10 weeks averaging at 35.48 g and 40.17 g, respectively (Fig 1, a,b and g,h). $ERR\alpha^{3SA}$ mice on a HFD or a HFD supplemented with fructose consumed similar amounts of calories, 93.76 and 95.97 kcal/mouse/week, despite difference in weight gain (Fig. 1, c and i and Table 1). Lastly, $ERR\alpha^{-/-}$ mice gained similar amounts of weight as WT on a HFD supplemented with fructose (Fig. 1, g,h) $ERR\alpha^{-/-}$ mice also had similar caloric intake to WT at 106.36 and 101.05 kcal/mouse/week, respectively (Fig. 1, i and Table 1).

Thus, $ERR\alpha$ mouse models on just a HFD with water gained weight in a similar manner to that recorded by Luo *et al.* On a HFD supplemented with glucose, $ERR\alpha^{-/-}$ mice were protected from diet induced obesity, and gained significantly less weight than WT and $ERR\alpha^{3SA}$ on the same diet and $ERR\alpha^{-/-}$ mice on just a HFD with water. On a HFD supplemented with fructose, $ERR\alpha^{3SA}$ mice also were protected from diet induced

obesity, and gained significantly less weight than WT and $ERR\alpha^{-/-}$ on the same diet and $ERR\alpha^{3SA}$ mice on just a HFD with water.

Sugar diet induced tissue weight changes in $ERR\alpha$ mouse models

After 10 weeks on their respective diets, WT, $ERR\alpha^{-/-}$ and $ERR\alpha^{3SA}$ mice were sacrificed, and the liver, epididymal white adipose tissue (eWAT), inguinal white adipose tissue (iWAT), gastrocnemius and soleus muscle mass were measured to assess where these mice were storing the excess weight (Fig. 2, a-o). Mice on a LFD supplemented with water showed no negligible difference in liver, eWAT, iWAT, gastrocnemius and soleus tissue mass between all three genotypes (Fig. 2, a,d,g,j,m). However, on a HFD supplemented with water, $ERR\alpha^{-/-}$ mice had smaller livers, slightly less gastrocnemius and soleus muscle mass but more eWAT and iWAT tissue (Fig. 2, a,d,g,j,m). Differences in tissue mass in $ERR\alpha^{3SA}$ mice were less severe on a HFD supplemented with water. Liver, gastrocnemius and soleus masses were similar to WT, and eWAT and iWAT masses trended towards being increased (Fig. 2, a,d,g,j,m).

Mice on a LFD supplemented with glucose had negligible differences in eWAT and iWAT weights between all three genotypes, however there were decreased trends seen in $ERR\alpha^{-/-}$ mice as compared to WT (not statistically significant) (Fig. 2, e,h). Liver, gastrocnemius and soleus in $ERR\alpha^{-/-}$ mice also trended downward compared to WT in this diet condition (Fig. 2, b,k,n). On a HFD supplemented with glucose, $ERR\alpha^{-/-}$ mice also had smaller livers, but less eWAT and iWAT, and similar gastrocnemius and soleus muscle mass to WT (Fig. 2, b,e,h,k,n). $ERR\alpha^{3SA}$ mice had similar organ weights to WT on both a LFD and HFD, which paralleled their overall weight gain (Fig. 2, b,e,h,k,n).

Mice on a LFD supplemented with fructose had no negligible differences in liver, eWAT, iWAT, gastrocnemius and soleus muscle mass between the three genotypes (Fig. 2, c,f,i,l,o). On a HFD supplemented with fructose, there was no significant decrease in liver, eWAT, iWAT, gastrocnemius and soleus mass between WT and $ERR\alpha^{3SA}$, despite decreased overall weight gain for the latter (Fig. 2, c,f,i,l,o). However there is a slight decrease in liver eWAT and soleus weight that was statistically

insignificant but might account for the decreased overall weight gain in $ERR\alpha^{3SA}$ (Fig. 2, f,o). Similar organ weights were seen in $ERR\alpha^{-/-}$ mice as compared to WT, as well (Fig. 2, c,f,i,l,o).

Overall, $ERR\alpha$ mouse models on a HFD supplemented with just water showed differential organ tissue weight gain. $ERR\alpha^{-/-}$ mice had small livers and more adipose tissue than WT, with similar muscle mass. Addition of glucose caused a decrease in adipose tissue mass, perhaps providing an explanation for why we observed decreased body weights at experimental endpoint compared to WT. $ERR\alpha^{3SA}$ mice showed similar organ weights to WT, but showed (statistically insignificant) decreases in liver, adipose and muscle mass weights. Overall, decreased organ weights in both genotypes mimic overall weight gain trends, with most drastic changes observed in liver and fat weights.

Sugar diet-induced changes in gross liver appearance full body lipid distribution in $ERR\alpha$ mouse models

To evaluate the weight distribution changes more clearly between liver and adipose tissue due to sugar supplementations in the $ERR\alpha$ mouse models, a correlation plot was made. WT mice fed LFD supplemented with water had average liver and adipose tissue weights of 1.26 g and 0.92 g, respectively (Fig. 3, a and Table 2). Supplementation with glucose or fructose caused similar increase in the liver weight but adipose tissue remains relatively unchanged (Fig. 3, a). The appearances of these livers also seemed paler than those observed on LFD with water (Fig. 4). $ERR\alpha^{-/-}$ mice on a LFD had decreased average liver and adipose tissue weights of 1.17 g and 0.49 g as compared to wildtype (Table 2). Supplementation with glucose or fructose on this diet increased adipose tissue, while liver weights and appearance remained relatively unchanged (Fig. 3, a and Fig. 4). On a HFD supplemented with water, WT mice had liver and adipose average tissue weights being 1.95 g and 1.72 g respectively. This represents an approximate equal increase of ~0.7 g in both organs compared to the LFD and can be visually identified in the liver by observing a paler complexion with fatty “spots” visible on the surface of the organ (Table 2 and Fig. 4). Supplementation with glucose or fructose to the HFD resulted in an additional approximate increase of ~0.7 g in

adipose tissue only and supported by similar fatty appearing liver (Table 2 and Fig. 4). Conversely, $ERR\alpha^{-/-}$ mice on a HFD had average liver and adipose tissue weights of 1.21 g and 3.09 g respectively (Fig. 3, a and Table 2). This represents a ~6-fold increase in adipose tissue weight from the LFD, while the liver weight remained relatively unchanged and its appearance still had a bright red hue (Table 2 and Fig. 4). Surprisingly, supplementation with fructose or glucose resulted in a decrease in adipose tissue mass for both sugars, and a slight increase in liver mass for fructose only (Fig. 3, a). This highlights that glucose supplementation to a high fat diet in $ERR\alpha^{-/-}$ mice seems uniquely protective compared to fructose, as it reduces adipose tissue and liver weights compared to WT.

ERR^{3SA} mice has similar liver mass and less adipose tissue compared to WT on a LFD supplemented with water, with weights of 1.38 g and 0.42 g respectively (Fig 3, b and Table 2). Contrary to WT and $ERR\alpha^{-/-}$ mice, supplementation with glucose and fructose to this diet caused a slight decreased liver mass but did not yield any significant changes to general liver appearance (Fig. 3, b and Fig. 4). On a HFD supplemented with water, ERR^{3SA} mice have liver and adipose weights of 1.69 g and 2.46 g respectively (Fig. 3, b). The surface of the liver contained the “fatty spots”, like WT mice (Fig. 4). Contrary to WT mice that had equal weight gain in both organs and $ERR\alpha^{-/-}$ mice who preferentially stored extra weight in only their adipose tissue, $ERR\alpha^{3SA}$ mice on a HFD gained preferential weight in their adipose tissue, but the liver was not completely protected. Supplementation with glucose and fructose on a HFD in $ERR\alpha^{3SA}$ mice also caused a slight decrease in adipose tissue mass for both sugars, similar to $ERR\alpha^{-/-}$ mice (Fig. 3, c). However, conversely to $ERR\alpha^{-/-}$ mice, only fructose supplementation on a HFD caused a decrease in the average liver weight to 1.94 g, with an accompanying liver appearance that was paler, with visible fat deposits (Fig. 3, c and Fig. 4).

Overall, the decreased adipose weight phenotype seen in $ERR\alpha^{-/-}$ and ERR^{3SA} mice fed a HFD supplemented with glucose and fructose, respectively, showed a retraction of the obesogenic weight gain caused by the HFD. Observation of gross liver appearances post dissection of $ERR\alpha^{-/-}$ mice fed a HFD supplemented with glucose or $ERR\alpha^{3SA}$ fed a HFD supplemented with fructose, displays livers that are paler than mice

that were just on a HFD, on a HFD with the opposite sugar or WT mice on the same diet.

Sugar Diet-induced changes in glucose homeostasis in $ERR\alpha$ mouse models

After 8 weeks on their respective diets, $ERR\alpha^{-/-}$, $ERR\alpha^{3SA}$ and WT fed a LFD or HFD, supplemented with water or sugar, were subjected to a GTT to assess how well glucose clearance and handling was. A bolus injection of 2 g/kg of glucose was done and glucose levels were measured periodically for two hours afterwards. An increased Area Under the Curve (AUC) during the GTT, corresponds to inefficient glucose clearance from the circulation by organ cells, and can be a sign of insulin resistance. On a LFD supplemented with water there were no significant differences in fasting glucose levels in all three genotypes (Fig. 5, a). On a HFD, this increased the fasting glucose of WT mice, but not significantly (Fig. 5, a). $ERR\alpha^{-/-}$ mice on a high fat diet did have a lower fasting glucose than WT, and slightly better glucose clearance during the GTT, although the final AUC was not statistically different than WT (Fig. 5, b,c). $ERR\alpha^{3SA}$ mice showed no differences in fasting glucose or glucose clearance during GTT, in low or high fat diets, compared to WT (Fig. 5, a,b,c).

On a LFD supplemented with glucose, WT mice had higher fasting glucose levels compared to just a LFD (Fig. 5, a.d). $ERR\alpha^{-/-}$ mice had decreased fasting glucose levels compared to WT and improved glucose clearance during GTT (Fig. 5 d,e,f). This trend was also seen in the HFD supplemented with glucose and is in line with the decreased body weight seen in this genotype. $ERR\alpha^{3SA}$ also had lower fasting glucose levels compared to WT but shown no significant difference during the GTT (Fig. 5, d,e,f). On a HFD supplemented with glucose, $ERR\alpha^{3SA}$ displayed the highest fasting glucose, but no significant changes in glucose clearance during GTT as compared to WT (Fig. 5, d,e,f).

On a LFD supplemented with fructose, all three genotypes showed no significant differences in fasting glucose levels, however $ERR\alpha^{-/-}$ mice did have better glucose tolerance during GTT as compared to WT (Fig. 5 g,h,i). A HFD supplemented with fructose also showed no significant differences between genotypes (Fig. 5 g,h,i).

Overall, we observed improved glucose tolerance in $ERR\alpha^{-/-}$ mice fed a HFD supplemented with glucose, but no difference in $ERR\alpha^{3SA}$ mice fed a HFD supplemented with fructose, despite weight trends.

Sugar diet induced changes in insulin homeostasis in $ERR\alpha$ mouse models

Further evaluation into $ERR\alpha$ mouse models involved assessing their insulin sensitivity during an ITT test, also after 8 weeks on their respective diets. Through bolus injection of insulin, glucose decay readings were taken sequentially for two hours afterwards. A higher AUC value for an ITT test that the injected insulin was inefficient in clearing insulin from circulation, resulting in higher plasma glucose levels and insulin resistance.

A LFD supplemented with water, glucose or fructose, did not show any significant changes in glucose decay during ITT or AUC values, between all three genotypes (Fig. 6). However on the HFD supplemented with only water, the $ERR\alpha^{-/-}$ displayed the most sensitivity to insulin, as the AUC value dropped by nearly half of that of WT and $ERR\alpha^{3SA}$ (Fig. 6 a,b). HFDs supplemented with glucose or fructose did not show any significant differences in insulin sensitivity for the three genotypes.

Figure 1: Diet induced weight gain in $ERR\alpha^{-/-}$, $ERR\alpha^{3SA}$ and their wildtype controls. Starting at 6 weeks of age, male $ERR\alpha^{-/-}$, $ERR\alpha^{3SA}$ and WT mice were fed a low-fat control diet (LFD), or a high-fat diet (HFD), supplemented with regular water, 30% glucose solution or 30% fructose solution. (a,d,g) Average body weights with water (a), glucose (d) or fructose (g) supplementation for 10 weeks on respective diets. (b,e,h) Average body weights at experimental endpoint of 10 weeks with water (b), glucose (e) or fructose (h) supplementation. Total caloric intake from both solid food and liquid was measured weekly for 10 weeks. Data are means \pm SEM, n= 9-12 mice per diet group. * $P < 0.05$, ** $P < 0.01$, *** $P < 0.001$ assessed by unpaired t test. WT, wildtype; KO, $ERR\alpha^{-/-}$; 3SA, $ERR\alpha^{3SA}$.

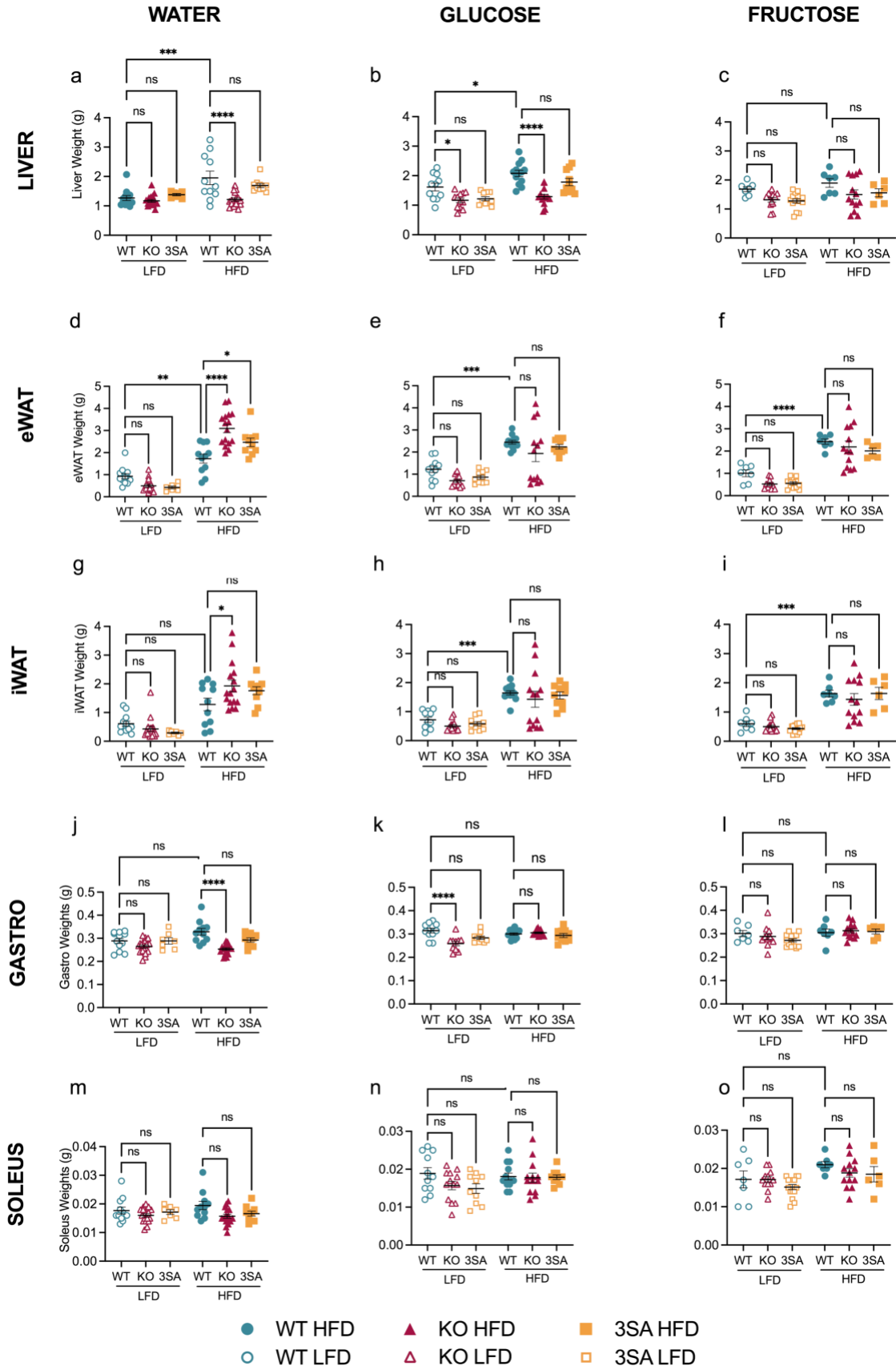


Figure 2: Diet-induced weight changes in liver, adipose tissue and skeletal muscle in $ERR\alpha^{-/-}$, $ERR\alpha^{3SA}$ and their wildtype controls. Tissue composition in wildtype (blue circles), $ERR\alpha^{-/-}$ (red triangles), and $ERR\alpha^{3SA}$ (yellow squares), fed a low fat control diet (LFD, open symbols) or high fat diet (HFD, closed symbols), supplemented with regular water, 30% glucose solution or 30% fructose solution, for 10 weeks. The mice were first weighed pre sacrifice, the livers (a,b,c) , epididymal white fat (eWAT) (d,e,f), inguinal white fat (iWAT) (g,h,i), gastrocnemius (j,k,l) and soleus (m,n,o) muscle were dissected and weighed. Data are means \pm SEM, n= 9-12 mice per diet group. * $P < 0.05$, ** $P < 0.01$, *** $P < 0.001$ assessed by one way ANOVA with post hoc Tukey's test. WT, wildtype; KO, $ERR\alpha^{-/-}$; 3SA, $ERR\alpha^{3SA}$; LFD.

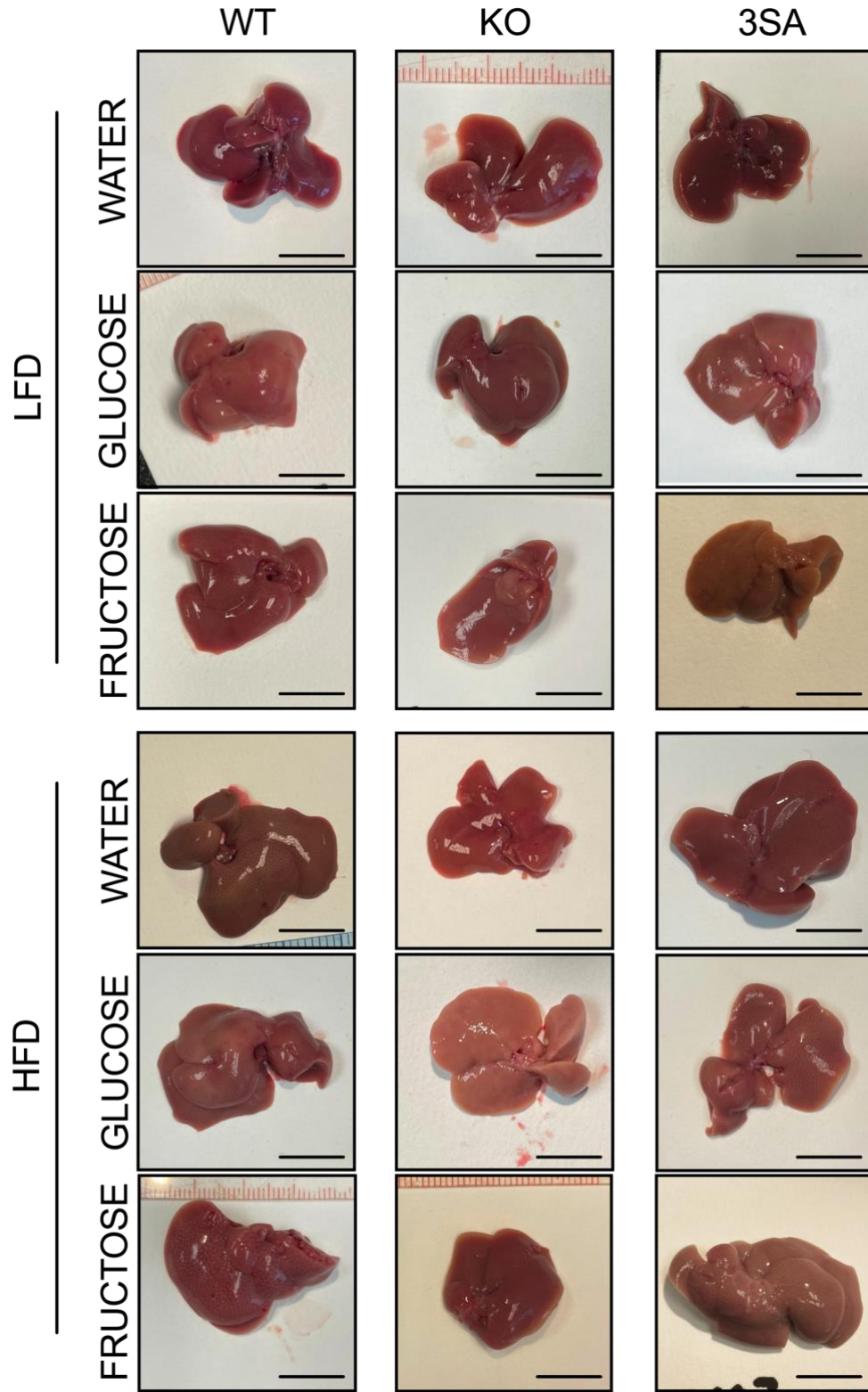


Figure 3: Diet-induced changes in gross liver appearance in $ERR\alpha^{-/-}$, $ERR\alpha^{3SA}$ and their wildtype controls. Representative appearance of the liver in wildtype, $ERR\alpha^{-/-}$, and $ERR\alpha^{3SA}$, fed a low-fat control diet (LFD) or high fat diet (HFD, closed symbols), supplemented with regular water, 30% glucose solution or 30% fructose solution, for 10 weeks with n= 9-12 mice per diet group. Scale bars represent 10 mm. WT, wildtype; KO, $ERR\alpha^{-/-}$; 3SA, $ERR\alpha^{3SA}$.

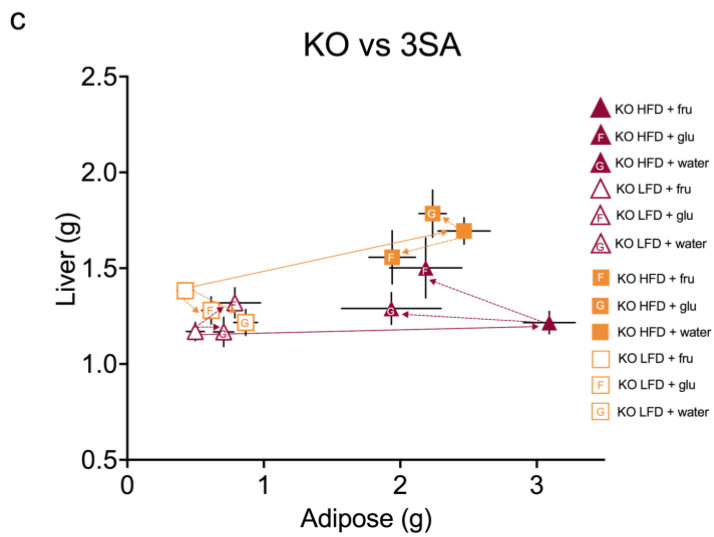
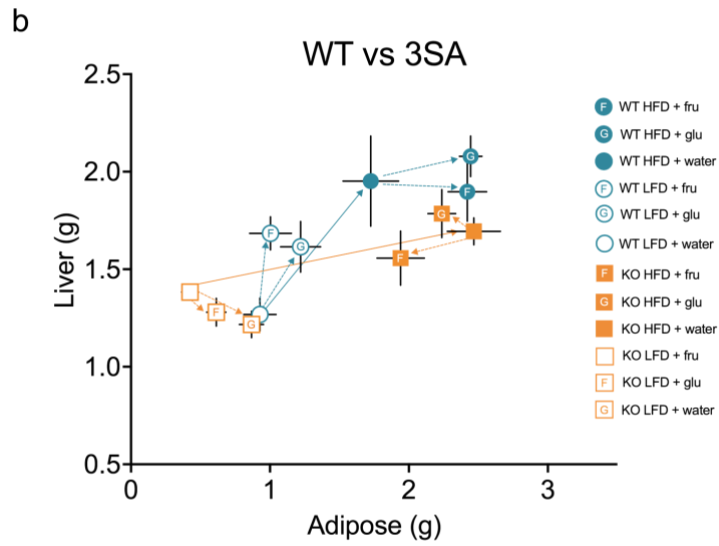
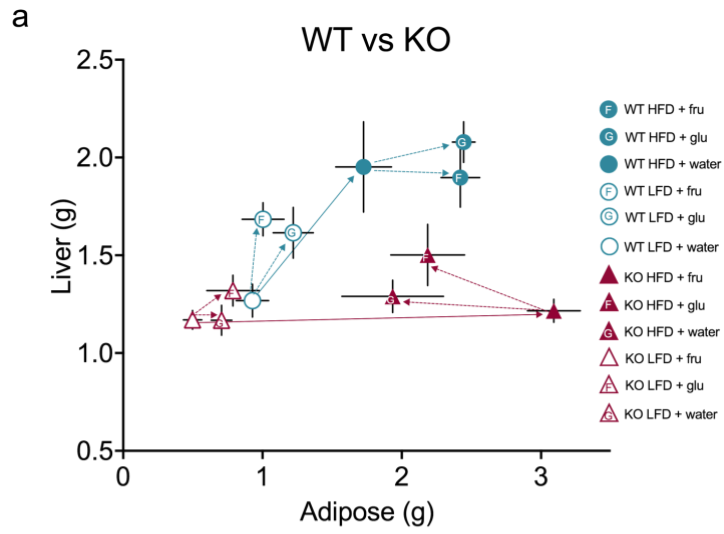
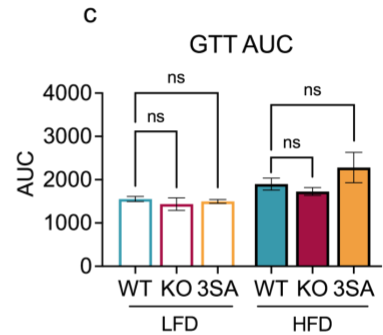
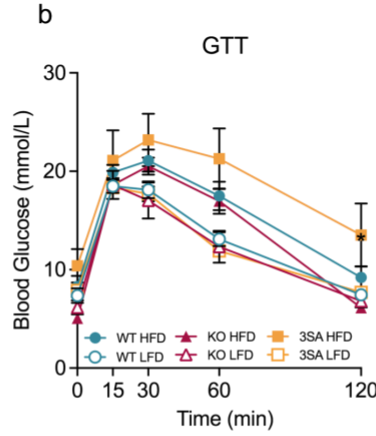
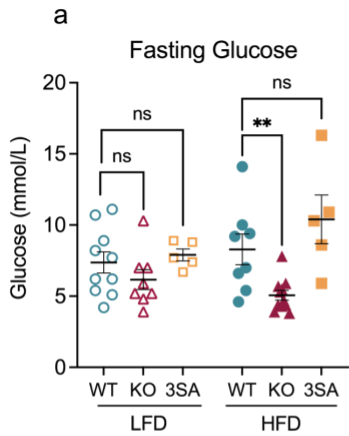
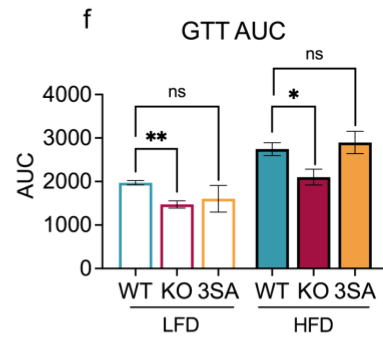
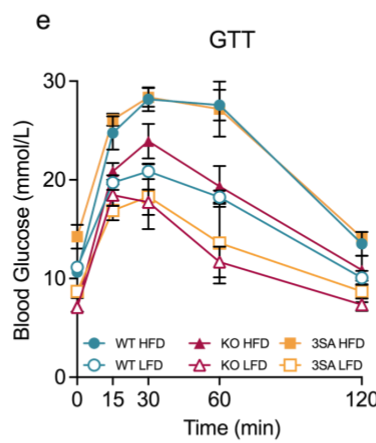
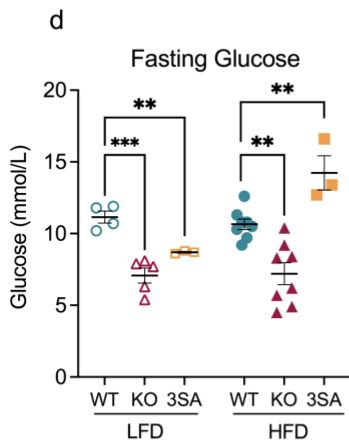


Figure 4: Diet-induced changes in lipid distribution in $ERR\alpha^{-/-}$, $ERR\alpha^{3SA}$ and their wildtype controls. Liver and epididymal adipose tissue (eWAT) weight composition in male wildtype (blue circles), $ERR\alpha$ KO (red triangles), and $ERR\alpha^{3SA}$ (yellow squares), fed a low-fat control diet (LFD, open symbols) or high fat diet (HFD, closed symbols), supplemented with regular water, 30% glucose solution or 30% fructose solution, for 10 weeks. Comparisons of liver vs adipose tissue between WT vs $ERR\alpha^{-/-}$ (a), WT vs $ERR\alpha^{3SA}$ (b) and $ERR\alpha^{-/-}$ vs $ERR\alpha^{3SA}$ (c) in separate plots. Data are means \pm SEM, n= 9-12 mice per diet group. Arrows for clarity in following diet condition. WT, wildtype; KO, $ERR\alpha^{-/-}$; 3SA, $ERR\alpha^{3SA}$; F, fructose; G, glucose.

WATER



GLUCOSE



FRUCTOSE

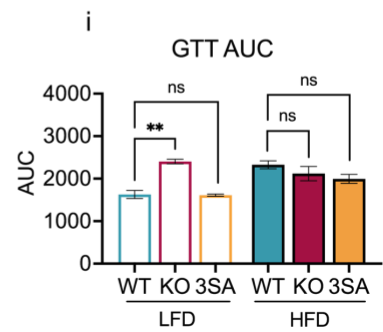
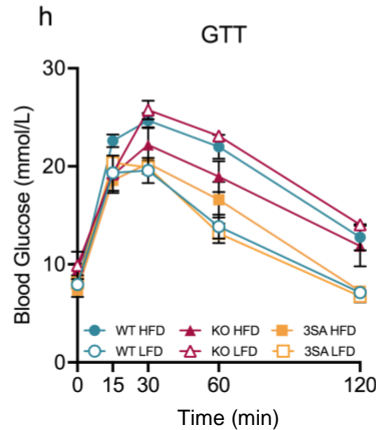
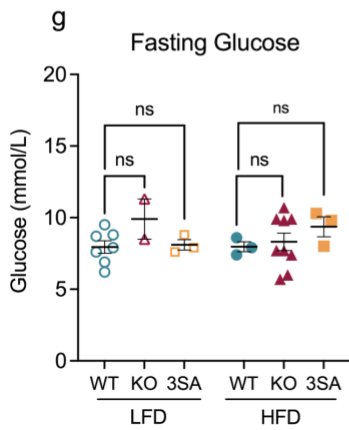


Figure 5: Diet-induced changes in glucose homeostasis in $ERR\alpha^{-/-}$, $ERR\alpha^{3SA}$ and their wildtype controls. Starting at 6 weeks of age, male WT (blue circles), $ERR\alpha^{-/-}$ (red triangles) and $ERR\alpha^{3SA}$ (yellow squares) were fed a low fat control diet (LFD, open symbol), or a high fat diet (HFD, closed symbol), supplemented with regular water (a,b,c), 30% glucose solution (d,e,f) or 30% fructose solution (g,h,i). After 8 weeks on their respective diets, glucose homeostasis was assessed. Fasting glucose levels in male mice fed water (a), glucose (d) or fructose (g). Glucose tolerance tests were performed in male mice fed water (b), glucose (e) or fructose (h), and average changes in blood glucose were recorded at 0, 15-, 30-, 60- and 120-minutes following bolus injection of glucose (2g/kg). Average area under the curve for GTT data in male mice fed water (c), glucose (f) or fructose (i). Data are means \pm SEM, n = 2-8 mice per group, * $P < 0.05$, ** $P < 0.01$, *** $P < 0.001$ assessed by one way ANOVA with post hoc Tukey's test. AUC, Area Under the Curve; WT, wildtype; KO, $ERR\alpha^{-/-}$; 3SA, $ERR\alpha^{3SA}$.

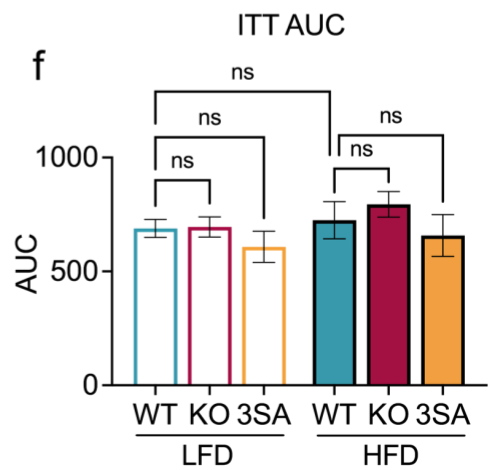
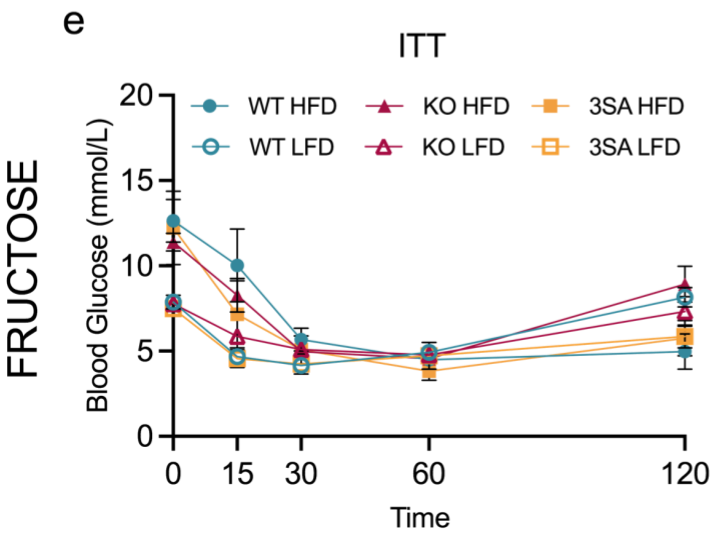
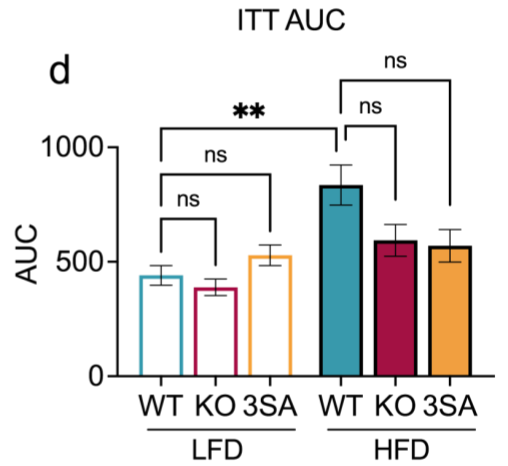
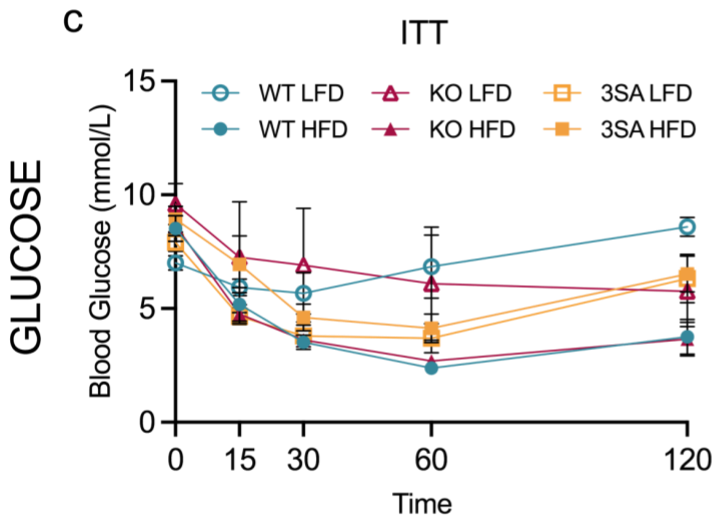
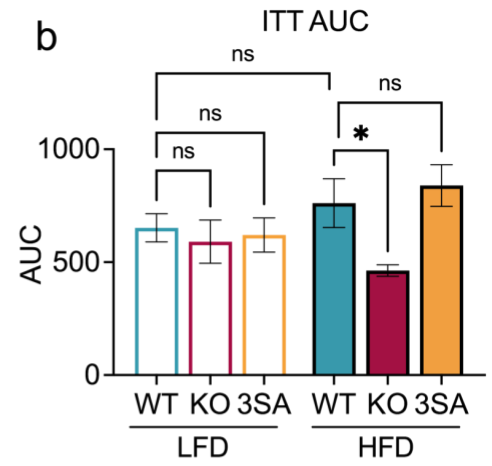
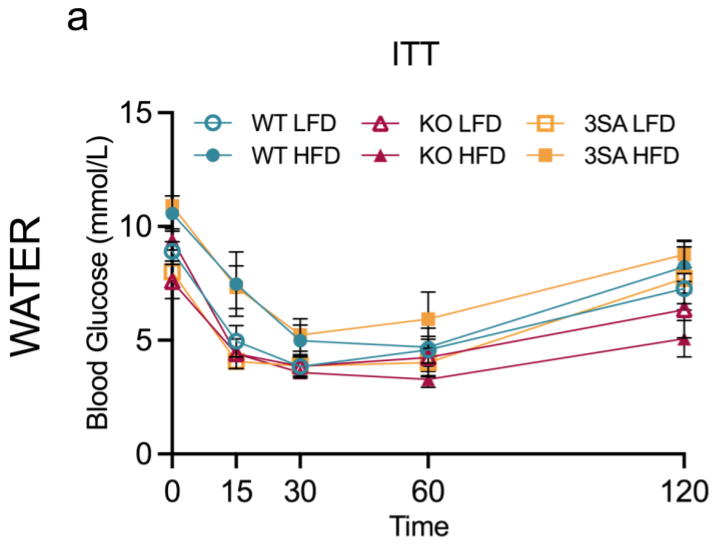


Figure 6: Diet-induced changes in insulin homeostasis in $ERR\alpha^{-/-}$, $ERR\alpha^{3SA}$ and their wildtype controls. Starting at 6 weeks of age, male WT (blue circles), $ERR\alpha^{-/-}$ (red triangles) and $ERR\alpha^{3SA}$ (yellow squares) were fed a low fat control diet (LFD, open symbol), or a high fat diet (HFD, closed symbol), supplemented with regular water (a,b,c), 30% glucose solution (d,e,f) or 30% fructose solution (g,h,i). After 8 weeks on their respective diets, insulin homeostasis was assessed. Insulin tolerance tests were performed in male mice fed water (a), glucose (c) or fructose (e), and average changes in blood glucose were recorded at 0, 15, 30, 60 and 120 min, following bolus injection of 0.75U/kg or 2U/kg, for LFD or HFD fed mice, respectively. Average area under the curve for ITT data in male mice fed water (b), glucose (d) or fructose (f). Data are means \pm SEM, n = 2-8 mice per group, * $P < 0.05$, ** $P < 0.01$, *** $P < 0.001$ assessed by one way ANOVA with post hoc Tukey's test. AUC, Area Under the Curve; WT, wildtype; KO, $ERR\alpha^{-/-}$; 3SA, $ERR\alpha^{3SA}$.

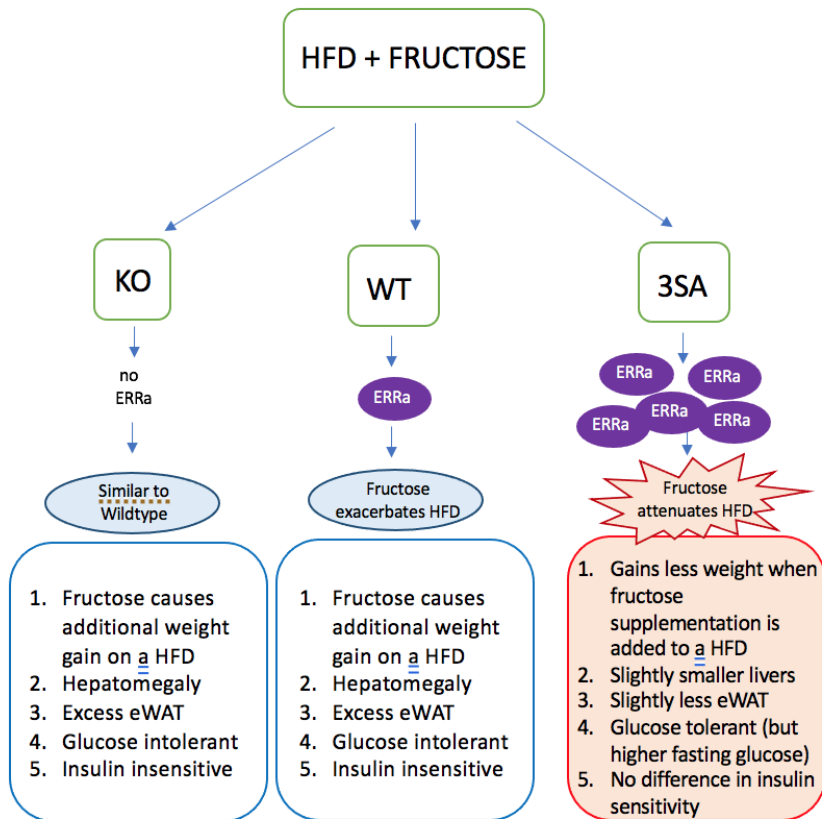
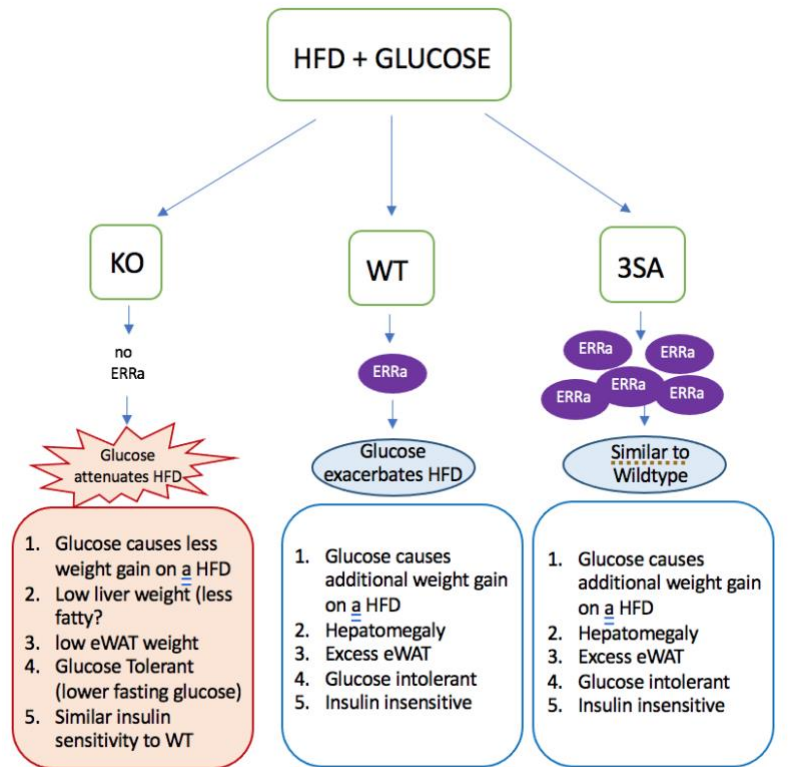


Figure 7: Flow chart summarizing comparisons of diet induced changes between WT, $ERR\alpha^{-/-}$ and $ERR\alpha^{3SA}$ mice. Male WT, $ERR\alpha^{-/-}$ and $ERR\alpha^{3SA}$ mice were fed a low-fat diet (LFD) or a high-fat diet (HFD) diet supplemented with water, 30% glucose or 30% fructose, starting at 6 weeks of age for 10 weeks. The chart highlights sugar-induced metabolic differences in $ERR\alpha^{-/-}$ and $ERR\alpha^{3SA}$ compared with their WT controls. WT, wildtype; KO, $ERR\alpha^{-/-}$; 3SA, $ERR\alpha^{3SA}$.

WT	LFD	water	81.51
		glucose	95.67
		fructose	77.56
	HFD	water	104.14
		glucose	106.91
		fructose	101.05
ERR α ^{-/-}	LFD	water	73.57
		glucose	93.04
		fructose	76.21
	HFD	water	93.04
		glucose	103.00
		fructose	106.36
ERR α ^{3SA}	LFD	water	81.20
		glucose	102.48
		fructose	89.86
	HFD	water	95.97
		glucose	105.43
		fructose	93.76

Table 1: Total (pellet and liquid) weekly caloric (kcal) consumption per mouse.

			Liver	Adipose
WT	LFD	water	1.267 ± 0.084	0.928 ± 0.116
		glucose	1.615 ± 0.130	1.221 ± 0.144
		fructose	1.683 ± 0.085	1.004 ± 0.150
	HFD	water	1.951 ± 0.231	1.726 ± 0.200
		glucose	2.079 ± 0.104	2.445 ± 0.081
		fructose	1.896 ± 0.151	2.421 ± 0.139
ERR α ^{-/-}	LFD	water	1.170 ± 0.048	0.498 ± 0.066
		glucose	1.167 ± 0.077	0.706 ± 0.074
		fructose	1.318 ± 0.079	0.788 ± 0.188
	HFD	water	1.215 ± 0.059	3.092 ± 0.190
		glucose	1.290 ± 0.083	1.935 ± 0.365
		fructose	1.501 ± 0.157	2.186 ± 0.265
ERR α ^{3SA}	LFD	water	1.382 ± 0.038	0.425 ± 0.061
		glucose	1.217 ± 0.068	0.867 ± 0.087
		fructose	1.279 ± 0.071	0.614 ± 0.069
	HFD	water	1.693 ± 0.069	2.468 ± 0.191
		glucose	1.784 ± 0.123	2.237 ± 0.100
		fructose	1.556 ± 0.139	1.941 ± 0.170

Table 2: Liver and adipose tissue weights per diet condition. Data is represented as averages followed by ± SEM

XII. DISCUSSION

The transcriptional activity of the orphan nuclear receptor $ERR\alpha$ has been well characterized in the context of several metabolic and bioenergetic pathways within the liver, including lipid handling, insulin signaling, mitochondrial function as well as glucose homeostasis⁹⁴. In the absence of a natural ligand known to modulate the activity of $ERR\alpha$ in a physiological setting, our group has genetically modified mouse models coupled with transcriptomic approaches such as RNA-seq and ChIP-seq to reveal the long-term metabolic changes in transcription observed in the absence or over-abundance of the $ERR\alpha$ protein. As such, $ERR\alpha$ has been found to play a dynamic role in carbohydrate handling, specifically glucose homeostasis. However, its role in fructose metabolism has largely remained unexplored. A study published by Softic *et al.* in 2019 illustrated that fructose supplementation to a HFD was able to downregulate genes in FAO via three separate nodes of modulation. One of those, worked by reducing mitochondrial size and protein mass, causing a decrease in the rate of FAO. Fructose control of FAO in this context was suspected to be transcriptional in nature, as mRNA expression of FAO enzymes were downregulated after KHK knockdown. One hint that $ERR\alpha$ might play a role in the mitochondrial dysfunction observed during fructose supplementation was a compensatory upregulation of one of $PGC-1\alpha$, a well-known coregulator of $ERR\alpha$ transcriptional activity. We thus hypothesized that, in addition to other well-described external physiological stimuli, like cold exposure, calorie restriction and exercise, fructose consumption could also modulate the action of the $ERR\alpha/PGC-1\alpha$ transcriptional axis on energy metabolism. Indeed, the work described in this thesis shows that $ERR\alpha$ plays a divergent role in response to glucose and fructose consumption when supplemented together with a HFD.

A 10-week course of a LFD or HFD supplemented with water, 30% glucose or 30% fructose using a gain of function ($ERR\alpha^{3SA}$) or loss of functions ($ERR\alpha^{-/-}$) mouse model was administered to foster obesity related metabolic dysfunction and detangle some preliminary roles for $ERR\alpha$ in respect with the metabolic fate of these two sugars. In line with previous studies, both $ERR\alpha$ mouse models reacted to a HFD as expected^{129,144}.

The $ERR\alpha^{-/-}$ mouse model has already been well characterised and found to be resistant to HFD induced obesity on shorter regimens with reduced lipid content (5 vs 10 weeks: 45% vs 60%). On average, they are smaller than WT mice, but have the same amount of lean mass (~25% of total body weight).^{129,144} On a standard chow diet, their decreased weight is accounted for by diminished fat mass, which was seen in the eWAT and iWAT tissue masses as compared to WT (but was not statistically significant at the endpoint for this study). An interesting phenotype appears in these mice as well when a metabolic stressor such as a HFD is added. As previously mentioned, an early indicator of diabetes and a major risk factor for NAFLD is an impaired fasting glucose level. As such, previous literature and this experiment shows that $ERR\alpha^{-/-}$ mice have lower fasting glucose levels on a HFD as compared to WT (4.4-5.5 mmol/L) indicating prevention of a diabetic state. Although one of the simplest and easiest ways to measure liver fat content is through histological staining using Oil Red O, assessing average liver weight is a preliminary indicator of increased lipid content as well. The liver is one of the most metabolically flexible organs in the body and will accumulate and burn fat when the body demands it. However, when fat is chronically present, permanent accumulation of fat is known as steatosis (aka NAFLD). As replicated in this experiment, a striking phenotype is seen in $ERR\alpha^{-/-}$ mice on a HFD, in that $ERR\alpha$ loss spares the liver of additional weight gain (lipid stores) in favor of accumulating fat in visceral tissues such as eWAT and iWAT. Quantitatively, this is indicated by an almost 3-fold decrease in liver:adipose tissue ratio and qualitatively this can be observed by a gross liver appearance that maintains a red hue in $ERR\alpha^{-/-}$ mice livers. Overall, this observation indicates a protective phenotype against metabolic diseases, that normal WT are susceptible to. Supplementation of liquid glucose and fructose in WT mice appears to exacerbate the negative effects, especially on a HFD. However, the metabolically protective phenotype displayed by loss of $ERR\alpha$ is still in effect after sugar supplementation. In particular, HFD + glucose supplementation was particularly effective in preventing diet induced obesity, in that these mice gained less weight than even a HFD despite increased caloric intake. The $ERR\alpha^{-/-}$ mice had smaller livers than WT, as well as decreased adipose tissue weights. They also had better fasting glucose and glucose tolerance during a GTT. The $ERR\alpha^{-/-}$ mice showed a trend toward being

more sensitive to exogenous insulin injections than WT, however the AUC values were not statistically significant.

The $ERR\alpha^{3SA}$ model was developed by our laboratory to have mutations in three insulin sensitive phosphorylation sites in its NTD domain. Not only does this sever sensitivity to insulin signaling, but also causes $ERR\alpha$ to be protected against ubiquitin mediated proteasomal degradation, increasing whole body $ERR\alpha$ levels. As per previous experiments done by Xia *et al*, $ERR\alpha^{3SA}$ trend towards being slightly heavier than WT and the present experiment showed no statistical difference. These mice on a HFD are known for decreased glucose tolerance and insulin sensitivity during GTT and ITTs respectively. Concurrent with this, high fasting glucose, GTT AUC and ITT AUC values were seen in this experiment for HFD fed $ERR\alpha^{3SA}$ mice but were not statistically significant. The $ERR\alpha^{3SA}$ mice had bigger livers than WT on a HFD with more eWAT tissue mass, as seen in previous experiments with a longer regimen of HFD (10 weeks vs 17 weeks). Addition of liquid sugar supplementation to this diet mimicked what occurred with the $ERR\alpha^{-/-}$ mice. However, in the scenario of over-expression of $ERR\alpha$, a HFD supplemented with fructose provided the most protection against HFD-induced obesity. The $ERR\alpha^{3SA}$ mice gained less weight than WT mice on a HFD + fructose and even $ERR\alpha^{3SA}$ mice on just a HFD. Their liver and adipose tissue also trended towards decreased weights, although it was not statistically significant at this chosen endpoint. They displayed slightly higher fasting glucose but no differences in GTT AUC and ITT AUC values.

$ERR\alpha^{-/-}$ mice and $ERR\alpha^{3SA}$ mice fed a HFD with glucose or a HFD with fructose, respectively, might be protected from obesity and improve glucose tolerance (Fig. 7). However, upon observation of gross liver appearances, these organs are pale, have visible fat deposits, and have a “rippled” appearance. Traditional concerns surrounding obesity have all used the body mass index (BMI) as a criterion for overall health. The “adipose tissue expandability hypothesis” posits that every person’s adipose tissue has a maximal capacity to store lipids. This capacity varies within the population and is influenced by genetics or environmental factors. Once the adipose tissue has reached its expansion limit, lipids begin to “spill” into other organs causing lipotoxicity, adipokine

secretions and promoting insulin resistance. This is supported by lipodystrophy models, PPAR γ knockout studies and alterations in adipokine secretion followed saturated adipose tissue. It is this “spilling” that causes the associated metabolic conditions observed with obesity. However, reports of obese individuals who have evaded the expected weight related sequelae, termed “metabolically healthy obese” (MHO), have begun to surface. Currently the running classification for these individuals consist of having a BMI greater than 30 kg/m² and the absence of insulin resistance, hypertension or dyslipidemia. These individuals display distinct anthropometric phenotypes, most notably less visceral fat, and favorable inflammatory marker patterns. Conversely, some leaner individuals termed “metabolically unhealthy normal weight” (MUHNW) display metabolic abnormalities commonly seen in their obese counter parts. These are individuals with a BMI of less than 25 kg/m² and have increased risk for metabolic complications such as hyperinsulinemia, insulin resistance, hypertriglyceremia, coronary artery disease and lean-NAFLD. Often thinner individuals who are ‘metabolically unhealthy’ have worse outcomes and tend to progress into NASH and T2DM at a higher rate, likely due to increased abdominal fat distribution (high central adiposity). It is thought that MUHNW individual are susceptible to excessive metabolically active visceral adipose tissue, which is not always correlated to BMI.

The phenotypes of these two cohorts are of extreme interest to study in order to classify appropriate disease management. However, classification criteria have remained inconsistent. As such, total body weight or BMI are outdated measure to assess whether an individual is metabolically healthy or not. Development of MUHNW individuals has been largely attributed to diet quality rather than caloric overload, in that individuals adhering to a “western diet” high in processed sugars and fat posed most risk of developing the condition. As such, it is feasible to suggest that instead of being protected from HFD induced obesity, these two cohorts of mice, ERR α ^{-/-} fed HFD+glucose and ERR α ^{3SA} fed HFD+fructose, are transitioning from one type of metabolic syndrome to another, and that their weight loss and low liver weights are actually a sign of early deterioration. As previously mentioned, the presence or absence of ERR α can play a pathological or therapeutic role depending on the physiological context. It is thus it feasible that the absence of ERR α during excessive glucose loading

is detrimental, while fructose loading in the presence of ERR α could lead to a similar phenotype.

As a future direction for this project, it will be of interest to further delineated which specific pathways ERR α is regulating in these contexts. This study only uncovered the preliminary phenotypes, and several key experiments will need to be performed to assess whether the two above mentioned cohorts are protected by sugar diet induced obesity, or instead are gradually descending into a different metabolic disorder (one of leanness). Assessing the liver fat content, fibrosis and scarring with histological staining would be a preliminary step. Due to the profound changes to mitochondrial morphology previously described in HFD+fructose supplementation regimens, electron microscopy to assess hepatic mitochondria should be done, as well as *in vitro* Seahorse assays with primary hepatocytes to assess their mitochondrial function. RNA-seq of a subset of diet conditions to assess what hepatic transcriptional pathways are dysregulated would reveal global transcriptional changes that could provide hints to molecular mechanisms underlying these phenotypes. Lastly, additional mouse studies to include pharmacological inhibition of ERR α with C29 or fructose metabolism with KHK inhibition could be done to assure the specificity of action.

Previous reports of worse metabolic outcomes in male humans and mice have shown a clear association between worse metabolic outcome and sex, underscoring the importance of expanding the project in the future to include female mice as well. These additional mice were not included due to time constraints. Additionally cage littermates were not used for the same reason but backcrossing to reduce genetic background was done instead. Lastly, in all rodent studies using HFDs there is an additional amount of sucrose (sugar) within the pellet diet. It is impossible to completely eliminate it, as the pellets would not hold their shape. To alleviate this, the HFD and LFD used in this study was sucrose matched, in that it contained 8.9% in both to ensure that if mice consumed the same number of grams on either diet, they would be receiving the same number of calories from sucrose within the pellets.

Overall, this work enhances our understanding of the transcriptional activities of ERR α and lays the framework for studying its role in metabolizing to the two most commonly consumed sugar monomers, fructose and glucose. Depending on if ERR α is

attenuating or in fact worsening the effects of a HFD (based on whole body weight decreases in these categories), this could provide some therapeutic avenues for pharmacological inhibition or activation in humans to alleviate the effects of the Western diet. For example, if $ERR\alpha$ is attenuating the effects of a HFD supplemented with fructose, then SB 216763, a $Gsk3\beta$ inhibitor, would decrease the phosphorylation of its NTD and increase protein levels, ultimately being protective in humans who consume typically “unhealthy diets”. If loss of $ERR\alpha$ activity is beneficial for the body to handle excess glucose loading on a HFD, an $ERR\alpha$ inhibitor (or inverse agonist), such as C29 could be administered instead. However, if the opposite is true, and $ERR\alpha$ is actually causing these mice to become thinner, but ultimately metabolically unhealthier, the opposite drugs could be administered. However, this is complicated due to the fact that the two most common sweeteners HFCS and sucrose contain *both* glucose and fructose. Future studies in these mouse models using, for example, 30% sucrose water, could be more physiologically relevant for real world application.

XIII. CONCLUSION

Fructose consumption, especially in beverages, is characterized by the formation and accumulation of body fat, and its negative effects on public health is of major concern. This manuscript sought to delineated ERR α 's role in metabolizing this sugar as well as glucoses'. The primary aim was to characterize any phenotypic differences seen in between a gain or loss of function ERR α mouse models, and here we demonstrate that coupled with a HFD, these sugars cause differential patterns in overall weight gain, lipid distribution, glucose tolerance and insulin sensitivity. Ultimately, the initial aim of this study was met, and it provides further rationale to continue investigations into other aims such as uncovering the specific hepatic transcriptional programs activated or repressed by ERR α in this context using RNA-Seq or assessing mitochondrial morphology and function using electron microscopy. Additional studies and investigations into using other sugar compounds such as sucrose, or studying ERR α role in female mice, is merited.

Understanding the environmental contributors, pathophysiology and disease progression of metabolic disorders such as NAFLD, diabetes and obesity paves the way for personalized dietary recommendations for these individuals and could eventually improve their quality of life without the need for invasive surgeries.

REFERENCES

- 1 Ratziu, V., Goodman, Z. & Sanyal, A. Current efforts and trends in the treatment of NASH. *J Hepatol* **62**, S65-75, doi:10.1016/j.jhep.2015.02.041 (2015).
- 2 Ludwig, J., Viggiano, T. R., McGill, D. B. & Oh, B. J. Nonalcoholic steatohepatitis: Mayo Clinic experiences with a hitherto unnamed disease. *Mayo Clin Proc* **55**, 434-438 (1980).
- 3 Chalasani, N. *et al.* The diagnosis and management of non-alcoholic fatty liver disease: practice guideline by the American Gastroenterological Association, American Association for the Study of Liver Diseases, and American College of Gastroenterology. *Gastroenterology* **142**, 1592-1609, doi:10.1053/j.gastro.2012.04.001 (2012).
- 4 Gan, S. K. & Watts, G. F. Is adipose tissue lipolysis always an adaptive response to starvation?: implications for non-alcoholic fatty liver disease. *Clin Sci (Lond)* **114**, 543-545, doi:10.1042/CS20070461 (2008).
- 5 Schwimmer, J. B. *et al.* Prevalence of fatty liver in children and adolescents. *Pediatrics* **118**, 1388-1393, doi:10.1542/peds.2006-1212 (2006).
- 6 Hyysalo, J. *et al.* A population-based study on the prevalence of NASH using scores validated against liver histology. *J Hepatol* **60**, 839-846, doi:10.1016/j.jhep.2013.12.009 (2014).
- 7 Friedman, S. L. Hepatic stellate cells: protean, multifunctional, and enigmatic cells of the liver. *Physiol Rev* **88**, 125-172, doi:10.1152/physrev.00013.2007 (2008).
- 8 Lee, U. E. & Friedman, S. L. Mechanisms of hepatic fibrogenesis. *Best Pract Res Clin Gastroenterol* **25**, 195-206, doi:10.1016/j.bpg.2011.02.005 (2011).
- 9 Ellis, E. L. & Mann, D. A. Clinical evidence for the regression of liver fibrosis. *J Hepatol* **56**, 1171-1180, doi:10.1016/j.jhep.2011.09.024 (2012).
- 10 Kisseleva, T. *et al.* Myofibroblasts revert to an inactive phenotype during regression of liver fibrosis. *Proc Natl Acad Sci U S A* **109**, 9448-9453, doi:10.1073/pnas.1201840109 (2012).
- 11 Troeger, J. S. *et al.* Deactivation of hepatic stellate cells during liver fibrosis resolution in mice. *Gastroenterology* **143**, 1073-1083 e1022, doi:10.1053/j.gastro.2012.06.036 (2012).
- 12 Sivell, C. Nonalcoholic Fatty Liver Disease: A Silent Epidemic. *Gastroenterol Nurs* **42**, 428-434, doi:10.1097/sga.0000000000000443 (2019).
- 13 El-Serag, H. B. & Rudolph, K. L. Hepatocellular carcinoma: epidemiology and molecular carcinogenesis. *Gastroenterology* **132**, 2557-2576, doi:10.1053/j.gastro.2007.04.061 (2007).
- 14 Hanahan, D. & Weinberg, R. A. The hallmarks of cancer. *Cell* **100**, 57-70, doi:10.1016/s0092-8674(00)81683-9 (2000).
- 15 Virchow, R. Cellular pathology. As based upon physiological and pathological histology. Lecture XVI--Atheromatous affection of arteries. 1858. *Nutr Rev* **47**, 23-25, doi:10.1111/j.1753-4887.1989.tb02747.x (1989).
- 16 Ramakrishna, G. *et al.* From cirrhosis to hepatocellular carcinoma: new molecular insights on inflammation and cellular senescence. *Liver Cancer* **2**, 367-383, doi:10.1159/000343852 (2013).

- 17 Day, C. P. & James, O. F. Steatohepatitis: a tale of two "hits"? *Gastroenterology* **114**, 842-845, doi:10.1016/s0016-5085(98)70599-2 (1998).
- 18 Tilg, H., Moschen, A. R. & Roden, M. NAFLD and diabetes mellitus. *Nat Rev Gastroenterol Hepatol* **14**, 32-42, doi:10.1038/nrgastro.2016.147 (2017).
- 19 Ekstedt, M. *et al.* Long-term follow-up of patients with NAFLD and elevated liver enzymes. *Hepatology* **44**, 865-873, doi:10.1002/hep.21327 (2006).
- 20 McPherson, S. *et al.* Evidence of NAFLD progression from steatosis to fibrosing-steatohepatitis using paired biopsies: implications for prognosis and clinical management. *J Hepatol* **62**, 1148-1155, doi:10.1016/j.jhep.2014.11.034 (2015).
- 21 Wilcox, G. Insulin and insulin resistance. *Clin Biochem Rev* **26**, 19-39 (2005).
- 22 Kubota, T., Kubota, N. & Kadowaki, T. Imbalanced Insulin Actions in Obesity and Type 2 Diabetes: Key Mouse Models of Insulin Signaling Pathway. *Cell Metab* **25**, 797-810, doi:10.1016/j.cmet.2017.03.004 (2017).
- 23 Leavens, K. F. & Birnbaum, M. J. Insulin signaling to hepatic lipid metabolism in health and disease. *Crit Rev Biochem Mol Biol* **46**, 200-215, doi:10.3109/10409238.2011.562481 (2011).
- 24 Li, S., Brown, M. S. & Goldstein, J. L. Bifurcation of insulin signaling pathway in rat liver: mTORC1 required for stimulation of lipogenesis, but not inhibition of gluconeogenesis. *Proc Natl Acad Sci U S A* **107**, 3441-3446, doi:10.1073/pnas.0914798107 (2010).
- 25 Mu, W. *et al.* Potential Nexus of Non-alcoholic Fatty Liver Disease and Type 2 Diabetes Mellitus: Insulin Resistance Between Hepatic and Peripheral Tissues. *Front Pharmacol* **9**, 1566, doi:10.3389/fphar.2018.01566 (2018).
- 26 Perry, R. J., Samuel, V. T., Petersen, K. F. & Shulman, G. I. The role of hepatic lipids in hepatic insulin resistance and type 2 diabetes. *Nature* **510**, 84-91, doi:10.1038/nature13478 (2014).
- 27 Kumashiro, N. *et al.* Cellular mechanism of insulin resistance in nonalcoholic fatty liver disease. *Proc Natl Acad Sci U S A* **108**, 16381-16385, doi:10.1073/pnas.1113359108 (2011).
- 28 Petersen, M. C. *et al.* Insulin receptor Thr1160 phosphorylation mediates lipid-induced hepatic insulin resistance. *J Clin Invest* **126**, 4361-4371, doi:10.1172/JCI86013 (2016).
- 29 Samuel, V. T. *et al.* Inhibition of protein kinase Cepsilon prevents hepatic insulin resistance in nonalcoholic fatty liver disease. *J Clin Invest* **117**, 739-745, doi:10.1172/JCI30400 (2007).
- 30 Perry, R. J. *et al.* Leptin Mediates a Glucose-Fatty Acid Cycle to Maintain Glucose Homeostasis in Starvation. *Cell* **172**, 234-248 e217, doi:10.1016/j.cell.2017.12.001 (2018).
- 31 Krssak, M. *et al.* Intramyocellular lipid concentrations are correlated with insulin sensitivity in humans: a ¹H NMR spectroscopy study. *Diabetologia* **42**, 113-116, doi:10.1007/s001250051123 (1999).
- 32 Cline, G. W. *et al.* Impaired glucose transport as a cause of decreased insulin-stimulated muscle glycogen synthesis in type 2 diabetes. *N Engl J Med* **341**, 240-246, doi:10.1056/nejm199907223410404 (1999).
- 33 Rothman, D. L., Shulman, R. G. & Shulman, G. I. ³¹P nuclear magnetic resonance measurements of muscle glucose-6-phosphate. Evidence for reduced insulin-dependent

- muscle glucose transport or phosphorylation activity in non-insulin-dependent diabetes mellitus. *J Clin Invest* **89**, 1069-1075, doi:10.1172/jci115686 (1992).
- 34 Kim, J. K. *et al.* Glucose toxicity and the development of diabetes in mice with muscle-specific inactivation of GLUT4. *J Clin Invest* **108**, 153-160, doi:10.1172/JCI10294 (2001).
- 35 Petersen, K. F. *et al.* The role of skeletal muscle insulin resistance in the pathogenesis of the metabolic syndrome. *Proc Natl Acad Sci U S A* **104**, 12587-12594, doi:10.1073/pnas.0705408104 (2007).
- 36 Szendroedi, J. *et al.* Role of diacylglycerol activation of PKC θ in lipid-induced muscle insulin resistance in humans. *Proc Natl Acad Sci U S A* **111**, 9597-9602, doi:10.1073/pnas.1409229111 (2014).
- 37 Uyeda, K. & Repa, J. J. Carbohydrate response element binding protein, ChREBP, a transcription factor coupling hepatic glucose utilization and lipid synthesis. *Cell Metab* **4**, 107-110, doi:10.1016/j.cmet.2006.06.008 (2006).
- 38 Rabol, R., Petersen, K. F., Dufour, S., Flannery, C. & Shulman, G. I. Reversal of muscle insulin resistance with exercise reduces postprandial hepatic de novo lipogenesis in insulin resistant individuals. *Proc Natl Acad Sci U S A* **108**, 13705-13709, doi:10.1073/pnas.1110105108 (2011).
- 39 Mizuno, T. M., Funabashi, T., Kleopoulos, S. P. & Mobbs, C. V. Specific preservation of biosynthetic responses to insulin in adipose tissue may contribute to hyperleptinemia in insulin-resistant obese mice. *J Nutr* **134**, 1045-1050, doi:10.1093/jn/134.5.1045 (2004).
- 40 Wree, A., Kahraman, A., Gerken, G. & Canbay, A. Obesity affects the liver - the link between adipocytes and hepatocytes. *Digestion* **83**, 124-133, doi:10.1159/000318741 (2011).
- 41 Colditz, G. A. *et al.* Weight as a risk factor for clinical diabetes in women. *Am J Epidemiol* **132**, 501-513, doi:10.1093/oxfordjournals.aje.a115686 (1990).
- 42 Marchesini, G. *et al.* Association of nonalcoholic fatty liver disease with insulin resistance. *Am J Med* **107**, 450-455, doi:10.1016/s0002-9343(99)00271-5 (1999).
- 43 Kim, J. K., Gavrilova, O., Chen, Y., Reitman, M. L. & Shulman, G. I. Mechanism of insulin resistance in A-ZIP/F-1 fatless mice. *J Biol Chem* **275**, 8456-8460, doi:10.1074/jbc.275.12.8456 (2000).
- 44 Oral, E. A. *et al.* Leptin-replacement therapy for lipodystrophy. *N Engl J Med* **346**, 570-578, doi:10.1056/NEJMoa012437 (2002).
- 45 Carey, D. G., Jenkins, A. B., Campbell, L. V., Freund, J. & Chisholm, D. J. Abdominal fat and insulin resistance in normal and overweight women: Direct measurements reveal a strong relationship in subjects at both low and high risk of NIDDM. *Diabetes* **45**, 633-638, doi:10.2337/diab.45.5.633 (1996).
- 46 Petersen, K. F. *et al.* Reversal of nonalcoholic hepatic steatosis, hepatic insulin resistance, and hyperglycemia by moderate weight reduction in patients with type 2 diabetes. *Diabetes* **54**, 603-608, doi:10.2337/diabetes.54.3.603 (2005).
- 47 Goedeke, L. & Shulman, G. I. Therapeutic potential of mitochondrial uncouplers for the treatment of metabolic associated fatty liver disease and NASH. *Mol Metab* **46**, 101178, doi:10.1016/j.molmet.2021.101178 (2021).
- 48 United States. Congress. Senate. Select Committee on Nutrition and Human Needs. *Dietary goals for the United States*. (U.S. Govt. Print. Off., 1977).

- 49 La Berge, A. F. How the ideology of low fat conquered america. *J Hist Med Allied Sci* **63**, 139-177, doi:10.1093/jhmas/jrn001 (2008).
- 50 Popkin, B. M. & Nielsen, S. J. The sweetening of the world's diet. *Obes Res* **11**, 1325-1332, doi:10.1038/oby.2003.179 (2003).
- 51 Barlow, P., McKee, M., Basu, S. & Stuckler, D. Impact of the North American Free Trade Agreement on high-fructose corn syrup supply in Canada: a natural experiment using synthetic control methods. *CMAJ* **189**, E881-E887, doi:10.1503/cmaj.161152 (2017).
- 52 Riediger, N. D. & Clara, I. Prevalence of metabolic syndrome in the Canadian adult population. *CMAJ* **183**, E1127-1134, doi:10.1503/cmaj.110070 (2011).
- 53 Ford, E. S., Giles, W. H. & Dietz, W. H. Prevalence of the metabolic syndrome among US adults: findings from the third National Health and Nutrition Examination Survey. *JAMA* **287**, 356-359, doi:10.1001/jama.287.3.356 (2002).
- 54 Stanhope, K. L. Sugar consumption, metabolic disease and obesity: The state of the controversy. *Crit Rev Clin Lab Sci* **53**, 52-67, doi:10.3109/10408363.2015.1084990 (2016).
- 55 Allister Price, C. & Stanhope, K. L. Understanding the Impact of Added Sugar Consumption on Risk for Type 2 Diabetes. *J Calif Dent Assoc* **44**, 619-626 (2016).
- 56 Johnson, R. K. *et al.* Dietary sugars intake and cardiovascular health: a scientific statement from the American Heart Association. *Circulation* **120**, 1011-1020, doi:10.1161/CIRCULATIONAHA.109.192627 (2009).
- 57 DiMaggio, D. P. & Mattes, R. D. Liquid versus solid carbohydrate: effects on food intake and body weight. *Int J Obes Relat Metab Disord* **24**, 794-800, doi:10.1038/sj.ijo.0801229 (2000).
- 58 Herman, M. A. & Birnbaum, M. J. Molecular aspects of fructose metabolism and metabolic disease. *Cell Metab* **33**, 2329-2354, doi:10.1016/j.cmet.2021.09.010 (2021).
- 59 Taskinen, M. R. *et al.* Adverse effects of fructose on cardiometabolic risk factors and hepatic lipid metabolism in subjects with abdominal obesity. *J Intern Med* **282**, 187-201, doi:10.1111/joim.12632 (2017).
- 60 Stanhope, K. L. *et al.* Consuming fructose-sweetened, not glucose-sweetened, beverages increases visceral adiposity and lipids and decreases insulin sensitivity in overweight/obese humans. *J Clin Invest* **119**, 1322-1334, doi:10.1172/JCI37385 (2009).
- 61 Tappy, L. & Rosset, R. Fructose Metabolism from a Functional Perspective: Implications for Athletes. *Sports Med* **47**, 23-32, doi:10.1007/s40279-017-0692-4 (2017).
- 62 Pontzer, H. *et al.* Hunter-gatherer energetics and human obesity. *PLoS One* **7**, e40503, doi:10.1371/journal.pone.0040503 (2012).
- 63 Wright, E. M., Martín, M. G. & Turk, E. Intestinal absorption in health and disease--sugars. *Best Pract Res Clin Gastroenterol* **17**, 943-956, doi:10.1016/s1521-6918(03)00107-0 (2003).
- 64 Patel, C., Douard, V., Yu, S., Gao, N. & Ferraris, R. P. Transport, metabolism, and endosomal trafficking-dependent regulation of intestinal fructose absorption. *FASEB J* **29**, 4046-4058, doi:10.1096/fj.15-272195 (2015).
- 65 Zhao, S. *et al.* Dietary fructose feeds hepatic lipogenesis via microbiota-derived acetate. *Nature* **579**, 586-591, doi:10.1038/s41586-020-2101-7 (2020).

- 66 Francey, C. *et al.* The extra-splanchnic fructose escape after ingestion of a fructose-glucose drink: An exploratory study in healthy humans using a dual fructose isotope method. *Clin Nutr ESPEN* **29**, 125-132, doi:10.1016/j.clnesp.2018.11.008 (2019).
- 67 Bismut, H., Hers, H. G. & Van Schaftingen, E. Conversion of fructose to glucose in the rabbit small intestine. A reappraisal of the direct pathway. *Eur J Biochem* **213**, 721-726, doi:10.1111/j.1432-1033.1993.tb17812.x (1993).
- 68 Ginsburg, V. & Hers, H. G. On the conversion of fructose to glucose by guinea pig intestine. *Biochim Biophys Acta* **38**, 427-434, doi:10.1016/0006-3002(60)91278-6 (1960).
- 69 Jang, C. *et al.* The Small Intestine Converts Dietary Fructose into Glucose and Organic Acids. *Cell Metab* **27**, 351-361 e353, doi:10.1016/j.cmet.2017.12.016 (2018).
- 70 Dencker, H., Lunderquist, A., Meeuwisse, G., Norryd, C. & Tranberg, K. G. Absorption of fructose as measured by portal catheterization. *Scand J Gastroenterol* **7**, 701-705, doi:10.3109/00365527209180981 (1972).
- 71 Holdsworth, C. D. & Dawson, A. M. Absorption of Fructose in Man. *Proc Soc Exp Biol Med* **118**, 142-145, doi:10.3181/00379727-118-29780 (1965).
- 72 Jang, C. *et al.* The small intestine shields the liver from fructose-induced steatosis. *Nat Metab* **2**, 586-593, doi:10.1038/s42255-020-0222-9 (2020).
- 73 Heinz, F., Lamprecht, W. & Kirsch, J. Enzymes of fructose metabolism in human liver. *J Clin Invest* **47**, 1826-1832, doi:10.1172/JCI105872 (1968).
- 74 Oberhaensli, R. D., Galloway, G. J., Taylor, D. J., Bore, P. J. & Radda, G. K. Assessment of human liver metabolism by phosphorus-31 magnetic resonance spectroscopy. *Br J Radiol* **59**, 695-699, doi:10.1259/0007-1285-59-703-695 (1986).
- 75 Agius, L. Glucokinase and molecular aspects of liver glycogen metabolism. *Biochem J* **414**, 1-18, doi:10.1042/BJ20080595 (2008).
- 76 Petersen, K. F., Laurent, D., Yu, C., Cline, G. W. & Shulman, G. I. Stimulating effects of low-dose fructose on insulin-stimulated hepatic glycogen synthesis in humans. *Diabetes* **50**, 1263-1268, doi:10.2337/diabetes.50.6.1263 (2001).
- 77 Niculescu, L., Veiga-da-Cunha, M. & Van Schaftingen, E. Investigation on the mechanism by which fructose, hexitols and other compounds regulate the translocation of glucokinase in rat hepatocytes. *Biochem J* **321 (Pt 1)**, 239-246, doi:10.1042/bj3210239 (1997).
- 78 Taylor, S. R. *et al.* Dietary fructose improves intestinal cell survival and nutrient absorption. *Nature* **597**, 263-267, doi:10.1038/s41586-021-03827-2 (2021).
- 79 Donnelly, K. L. *et al.* Sources of fatty acids stored in liver and secreted via lipoproteins in patients with nonalcoholic fatty liver disease. *J Clin Invest* **115**, 1343-1351, doi:10.1172/JCI23621 (2005).
- 80 Lambert, J. E., Ramos-Roman, M. A., Browning, J. D. & Parks, E. J. Increased de novo lipogenesis is a distinct characteristic of individuals with nonalcoholic fatty liver disease. *Gastroenterology* **146**, 726-735, doi:10.1053/j.gastro.2013.11.049 (2014).
- 81 Kim, M. S. *et al.* ChREBP regulates fructose-induced glucose production independently of insulin signaling. *J Clin Invest* **126**, 4372-4386, doi:10.1172/JCI81993 (2016).
- 82 Iizuka, K., Bruick, R. K., Liang, G., Horton, J. D. & Uyeda, K. Deficiency of carbohydrate response element-binding protein (ChREBP) reduces lipogenesis as well as glycolysis. *Proc Natl Acad Sci U S A* **101**, 7281-7286, doi:10.1073/pnas.0401516101 (2004).

- 83 Ma, L., Robinson, L. N. & Towle, H. C. ChREBP*MLx is the principal mediator of glucose-induced gene expression in the liver. *J Biol Chem* **281**, 28721-28730, doi:10.1074/jbc.M601576200 (2006).
- 84 Eissing, L. *et al.* De novo lipogenesis in human fat and liver is linked to ChREBP-beta and metabolic health. *Nat Commun* **4**, 1528, doi:10.1038/ncomms2537 (2013).
- 85 Kursawe, R. *et al.* Decreased transcription of ChREBP-alpha/beta isoforms in abdominal subcutaneous adipose tissue of obese adolescents with prediabetes or early type 2 diabetes: associations with insulin resistance and hyperglycemia. *Diabetes* **62**, 837-844, doi:10.2337/db12-0889 (2013).
- 86 Erion, D. M. *et al.* The role of the carbohydrate response element-binding protein in male fructose-fed rats. *Endocrinology* **154**, 36-44, doi:10.1210/en.2012-1725 (2013).
- 87 Kim, M. *et al.* Intestinal, but not hepatic, ChREBP is required for fructose tolerance. *JCI Insight* **2**, doi:10.1172/jci.insight.96703 (2017).
- 88 Linden, A. G. *et al.* Interplay between ChREBP and SREBP-1c coordinates postprandial glycolysis and lipogenesis in livers of mice. *J Lipid Res* **59**, 475-487, doi:10.1194/jlr.M081836 (2018).
- 89 Mittendorfer, B., Yoshino, M., Patterson, B. W. & Klein, S. VLDL Triglyceride Kinetics in Lean, Overweight, and Obese Men and Women. *J Clin Endocrinol Metab* **101**, 4151-4160, doi:10.1210/jc.2016-1500 (2016).
- 90 Shimano, H. & Sato, R. SREBP-regulated lipid metabolism: convergent physiology - divergent pathophysiology. *Nat Rev Endocrinol* **13**, 710-730, doi:10.1038/nrendo.2017.91 (2017).
- 91 Curry, D. L. Effects of mannose and fructose on the synthesis and secretion of insulin. *Pancreas* **4**, 2-9, doi:10.1097/00006676-198902000-00002 (1989).
- 92 Softic, S. *et al.* Dietary Sugars Alter Hepatic Fatty Acid Oxidation via Transcriptional and Post-translational Modifications of Mitochondrial Proteins. *Cell Metab* **30**, 735-753 e734, doi:10.1016/j.cmet.2019.09.003 (2019).
- 93 Giguere, V. Transcriptional control of energy homeostasis by the estrogen-related receptors. *Endocr Rev* **29**, 677-696, doi:10.1210/er.2008-0017 (2008).
- 94 Xia, H., Dufour, C. R. & Giguere, V. ERRalpha as a Bridge Between Transcription and Function: Role in Liver Metabolism and Disease. *Front Endocrinol (Lausanne)* **10**, 206, doi:10.3389/fendo.2019.00206 (2019).
- 95 Giguere, V., Tremblay, A. & Tremblay, G. B. Estrogen receptor beta: re-evaluation of estrogen and antiestrogen signaling. *Steroids* **63**, 335-339, doi:10.1016/s0039-128x(98)00024-5 (1998).
- 96 Giguere, V., Yang, N., Segui, P. & Evans, R. M. Identification of a new class of steroid hormone receptors. *Nature* **331**, 91-94, doi:10.1038/331091a0 (1988).
- 97 Villena, J. A. & Kralli, A. ERRalpha: a metabolic function for the oldest orphan. *Trends Endocrinol Metab* **19**, 269-276, doi:10.1016/j.tem.2008.07.005 (2008).
- 98 Tremblay, A. M. & Giguere, V. The NR3B subgroup: an ovERRview. *Nucl Recept Signal* **5**, e009, doi:10.1621/nrs.05009 (2007).
- 99 Vu, E. H., Kraus, R. J. & Mertz, J. E. Phosphorylation-dependent sumoylation of estrogen-related receptor alpha1. *Biochemistry* **46**, 9795-9804, doi:10.1021/bi700316g (2007).

- 100 Tremblay, A. M., Wilson, B. J., Yang, X. J. & Giguere, V. Phosphorylation-dependent sumoylation regulates estrogen-related receptor-alpha and -gamma transcriptional activity through a synergy control motif. *Mol Endocrinol* **22**, 570-584, doi:10.1210/me.2007-0357 (2008).
- 101 Iniguez-Lluhi, J. A. & Pearce, D. A common motif within the negative regulatory regions of multiple factors inhibits their transcriptional synergy. *Mol Cell Biol* **20**, 6040-6050, doi:10.1128/MCB.20.16.6040-6050.2000 (2000).
- 102 Sladek, R., Bader, J. A. & Giguere, V. The orphan nuclear receptor estrogen-related receptor alpha is a transcriptional regulator of the human medium-chain acyl coenzyme A dehydrogenase gene. *Mol Cell Biol* **17**, 5400-5409, doi:10.1128/MCB.17.9.5400 (1997).
- 103 Dufour, C. R. *et al.* Genome-wide orchestration of cardiac functions by the orphan nuclear receptors ERRalpha and gamma. *Cell Metab* **5**, 345-356, doi:10.1016/j.cmet.2007.03.007 (2007).
- 104 Huppunen, J. & Aarnisalo, P. Dimerization modulates the activity of the orphan nuclear receptor ERRgamma. *Biochem Biophys Res Commun* **314**, 964-970, doi:10.1016/j.bbrc.2003.12.194 (2004).
- 105 Gearhart, M. D., Holmbeck, S. M., Evans, R. M., Dyson, H. J. & Wright, P. E. Monomeric complex of human orphan estrogen related receptor-2 with DNA: a pseudo-dimer interface mediates extended half-site recognition. *J Mol Biol* **327**, 819-832, doi:10.1016/s0022-2836(03)00183-9 (2003).
- 106 Barry, J. B., Laganier, J. & Giguere, V. A single nucleotide in an estrogen-related receptor alpha site can dictate mode of binding and peroxisome proliferator-activated receptor gamma coactivator 1alpha activation of target promoters. *Mol Endocrinol* **20**, 302-310, doi:10.1210/me.2005-0313 (2006).
- 107 Wilson, B. J., Tremblay, A. M., Deblois, G., Sylvain-Drolet, G. & Giguere, V. An acetylation switch modulates the transcriptional activity of estrogen-related receptor alpha. *Mol Endocrinol* **24**, 1349-1358, doi:10.1210/me.2009-0441 (2010).
- 108 Kallen, J. *et al.* Evidence for ligand-independent transcriptional activation of the human estrogen-related receptor alpha (ERRalpha): crystal structure of ERRalpha ligand binding domain in complex with peroxisome proliferator-activated receptor coactivator-1alpha. *J Biol Chem* **279**, 49330-49337, doi:10.1074/jbc.M407999200 (2004).
- 109 Greschik, H. *et al.* Structural and functional evidence for ligand-independent transcriptional activation by the estrogen-related receptor 3. *Mol Cell* **9**, 303-313, doi:10.1016/s1097-2765(02)00444-6 (2002).
- 110 Scholtes, C. & Giguere, V. Transcriptional control of energy metabolism by nuclear receptors. *Nat Rev Mol Cell Biol* **23**, 750-770, doi:10.1038/s41580-022-00486-7 (2022).
- 111 Rodgers, J. T. *et al.* Nutrient control of glucose homeostasis through a complex of PGC-1alpha and SIRT1. *Nature* **434**, 113-118, doi:10.1038/nature03354 (2005).
- 112 Jager, S., Handschin, C., St-Pierre, J. & Spiegelman, B. M. AMP-activated protein kinase (AMPK) action in skeletal muscle via direct phosphorylation of PGC-1alpha. *Proc Natl Acad Sci U S A* **104**, 12017-12022, doi:10.1073/pnas.0705070104 (2007).
- 113 Vega, R. B. & Kelly, D. P. A role for estrogen-related receptor alpha in the control of mitochondrial fatty acid beta-oxidation during brown adipocyte differentiation. *J Biol Chem* **272**, 31693-31699, doi:10.1074/jbc.272.50.31693 (1997).

- 114 Puigserver, P. *et al.* A cold-inducible coactivator of nuclear receptors linked to adaptive thermogenesis. *Cell* **92**, 829-839, doi:10.1016/s0092-8674(00)81410-5 (1998).
- 115 Emmett, M. J. *et al.* Histone deacetylase 3 prepares brown adipose tissue for acute thermogenic challenge. *Nature* **546**, 544-548, doi:10.1038/nature22819 (2017).
- 116 Huss, J. M., Kopp, R. P. & Kelly, D. P. Peroxisome proliferator-activated receptor coactivator-1alpha (PGC-1alpha) coactivates the cardiac-enriched nuclear receptors estrogen-related receptor-alpha and -gamma. Identification of novel leucine-rich interaction motif within PGC-1alpha. *J Biol Chem* **277**, 40265-40274, doi:10.1074/jbc.M206324200 (2002).
- 117 Schreiber, S. N., Knutti, D., Brogli, K., Uhlmann, T. & Kralli, A. The transcriptional coactivator PGC-1 regulates the expression and activity of the orphan nuclear receptor estrogen-related receptor alpha (ERRalpha). *J Biol Chem* **278**, 9013-9018, doi:10.1074/jbc.M212923200 (2003).
- 118 Yan, M. *et al.* Chronic AMPK activation via loss of FLCN induces functional beige adipose tissue through PGC-1alpha/ERRalpha. *Genes Dev* **30**, 1034-1046, doi:10.1101/gad.281410.116 (2016).
- 119 Audet-Walsh, E. *et al.* The PGC-1alpha/ERRalpha Axis Represses One-Carbon Metabolism and Promotes Sensitivity to Anti-folate Therapy in Breast Cancer. *Cell Rep* **14**, 920-931, doi:10.1016/j.celrep.2015.12.086 (2016).
- 120 Mottis, A., Mouchiroud, L. & Auwerx, J. Emerging roles of the corepressors NCoR1 and SMRT in homeostasis. *Genes Dev* **27**, 819-835, doi:10.1101/gad.214023.113 (2013).
- 121 Perez-Schindler, J. *et al.* The corepressor NCoR1 antagonizes PGC-1alpha and estrogen-related receptor alpha in the regulation of skeletal muscle function and oxidative metabolism. *Mol Cell Biol* **32**, 4913-4924, doi:10.1128/MCB.00877-12 (2012).
- 122 Yamamoto, H. *et al.* NCoR1 is a conserved physiological modulator of muscle mass and oxidative function. *Cell* **147**, 827-839, doi:10.1016/j.cell.2011.10.017 (2011).
- 123 Rosenfeld, M. G., Lunyak, V. V. & Glass, C. K. Sensors and signals: a coactivator/corepressor/epigenetic code for integrating signal-dependent programs of transcriptional response. *Genes Dev* **20**, 1405-1428, doi:10.1101/gad.1424806 (2006).
- 124 Jo, Y. S. *et al.* Phosphorylation of the nuclear receptor corepressor 1 by protein kinase B switches its corepressor targets in the liver in mice. *Hepatology* **62**, 1606-1618, doi:10.1002/hep.27907 (2015).
- 125 Charest-Marcotte, A. *et al.* The homeobox protein Prox1 is a negative modulator of ERR{alpha}/PGC-1{alpha} bioenergetic functions. *Genes Dev* **24**, 537-542, doi:10.1101/gad.1871610 (2010).
- 126 Goto, T. *et al.* Liver-specific Prox1 inactivation causes hepatic injury and glucose intolerance in mice. *FEBS Lett* **591**, 624-635, doi:10.1002/1873-3468.12570 (2017).
- 127 Castet, A. *et al.* Receptor-interacting protein 140 differentially regulates estrogen receptor-related receptor transactivation depending on target genes. *Mol Endocrinol* **20**, 1035-1047, doi:10.1210/me.2005-0227 (2006).
- 128 Chaveroux, C. *et al.* Molecular and genetic crosstalks between mTOR and ERRalpha are key determinants of rapamycin-induced nonalcoholic fatty liver. *Cell Metab* **17**, 586-598, doi:10.1016/j.cmet.2013.03.003 (2013).

- 129 Luo, J. *et al.* Reduced fat mass in mice lacking orphan nuclear receptor estrogen-related receptor alpha. *Mol Cell Biol* **23**, 7947-7956, doi:10.1128/MCB.23.22.7947-7956.2003 (2003).
- 130 Brown, E. L. *et al.* Estrogen-Related Receptors Mediate the Adaptive Response of Brown Adipose Tissue to Adrenergic Stimulation. *iScience* **2**, 221-237, doi:10.1016/j.isci.2018.03.005 (2018).
- 131 Villena, J. A. *et al.* Orphan nuclear receptor estrogen-related receptor alpha is essential for adaptive thermogenesis. *Proc Natl Acad Sci U S A* **104**, 1418-1423, doi:10.1073/pnas.0607696104 (2007).
- 132 Dufour, C. R. *et al.* Genomic convergence among ERRalpha, PROX1, and BMAL1 in the control of metabolic clock outputs. *PLoS Genet* **7**, e1002143, doi:10.1371/journal.pgen.1002143 (2011).
- 133 Busch, B. B. *et al.* Identification of a selective inverse agonist for the orphan nuclear receptor estrogen-related receptor alpha. *J Med Chem* **47**, 5593-5596, doi:10.1021/jm049334f (2004).
- 134 Patch, R. J. *et al.* Indazole-based ligands for estrogen-related receptor alpha as potential anti-diabetic agents. *Eur J Med Chem* **138**, 830-853, doi:10.1016/j.ejmech.2017.07.015 (2017).
- 135 Patch, R. J. *et al.* Identification of diaryl ether-based ligands for estrogen-related receptor alpha as potential antidiabetic agents. *J Med Chem* **54**, 788-808, doi:10.1021/jm101063h (2011).
- 136 B'Chir, W. *et al.* Divergent Role of Estrogen-Related Receptor alpha in Lipid- and Fasting-Induced Hepatic Steatosis in Mice. *Endocrinology* **159**, 2153-2164, doi:10.1210/en.2018-00115 (2018).
- 137 Mao, L. *et al.* Discovery of JND003 as a New Selective Estrogen-Related Receptor alpha Agonist Alleviating Nonalcoholic Fatty Liver Disease and Insulin Resistance. *ACS Bio Med Chem Au* **2**, 282-296, doi:10.1021/acsbiomedchemau.1c00050 (2022).
- 138 Leto, D. & Saltiel, A. R. Regulation of glucose transport by insulin: traffic control of GLUT4. *Nat Rev Mol Cell Biol* **13**, 383-396, doi:10.1038/nrm3351 (2012).
- 139 Wende, A. R., Huss, J. M., Schaeffer, P. J., Giguere, V. & Kelly, D. P. PGC-1alpha coactivates PDK4 gene expression via the orphan nuclear receptor ERRalpha: a mechanism for transcriptional control of muscle glucose metabolism. *Mol Cell Biol* **25**, 10684-10694, doi:10.1128/MCB.25.24.10684-10694.2005 (2005).
- 140 Mootha, V. K. *et al.* Erralpha and Gabpa/b specify PGC-1alpha-dependent oxidative phosphorylation gene expression that is altered in diabetic muscle. *Proc Natl Acad Sci U S A* **101**, 6570-6575, doi:10.1073/pnas.0401401101 (2004).
- 141 Herzog, B. *et al.* Estrogen-related receptor alpha is a repressor of phosphoenolpyruvate carboxykinase gene transcription. *J Biol Chem* **281**, 99-106, doi:10.1074/jbc.M509276200 (2006).
- 142 Ichida, M., Nemoto, S. & Finkel, T. Identification of a specific molecular repressor of the peroxisome proliferator-activated receptor gamma Coactivator-1 alpha (PGC-1alpha). *J Biol Chem* **277**, 50991-50995, doi:10.1074/jbc.M210262200 (2002).

- 143 Schreiber, S. N. *et al.* The estrogen-related receptor alpha (ERRalpha) functions in PPARgamma coactivator 1alpha (PGC-1alpha)-induced mitochondrial biogenesis. *Proc Natl Acad Sci U S A* **101**, 6472-6477, doi:10.1073/pnas.0308686101 (2004).
- 144 Xia, H. *et al.* Insulin action and resistance are dependent on a GSK3beta-FBXW7-ERRalpha transcriptional axis. *Nat Commun* **13**, 2105, doi:10.1038/s41467-022-29722-6 (2022).
- 145 Park, S. *et al.* ERRalpha-Regulated Lactate Metabolism Contributes to Resistance to Targeted Therapies in Breast Cancer. *Cell Rep* **15**, 323-335, doi:10.1016/j.celrep.2016.03.026 (2016).
- 146 Fan, W. & Evans, R. PPARs and ERRs: molecular mediators of mitochondrial metabolism. *Curr Opin Cell Biol* **33**, 49-54, doi:10.1016/j.ceb.2014.11.002 (2015).
- 147 Eichner, L. J. & Giguere, V. Estrogen related receptors (ERRs): a new dawn in transcriptional control of mitochondrial gene networks. *Mitochondrion* **11**, 544-552, doi:10.1016/j.mito.2011.03.121 (2011).
- 148 Nie, Y. & Wong, C. Suppressing the activity of ERRalpha in 3T3-L1 adipocytes reduces mitochondrial biogenesis but enhances glycolysis and basal glucose uptake. *J Cell Mol Med* **13**, 3051-3060, doi:10.1111/j.1582-4934.2008.00382.x (2009).
- 149 Cho, Y., Hazen, B. C., Russell, A. P. & Kralli, A. Peroxisome proliferator-activated receptor gamma coactivator 1 (PGC-1)- and estrogen-related receptor (ERR)-induced regulator in muscle 1 (Perm1) is a tissue-specific regulator of oxidative capacity in skeletal muscle cells. *J Biol Chem* **288**, 25207-25218, doi:10.1074/jbc.M113.489674 (2013).
- 150 Soriano, F. X. *et al.* Evidence for a mitochondrial regulatory pathway defined by peroxisome proliferator-activated receptor-gamma coactivator-1 alpha, estrogen-related receptor-alpha, and mitofusin 2. *Diabetes* **55**, 1783-1791, doi:10.2337/db05-0509 (2006).
- 151 Cartoni, R. *et al.* Mitofusins 1/2 and ERRalpha expression are increased in human skeletal muscle after physical exercise. *J Physiol* **567**, 349-358, doi:10.1113/jphysiol.2005.092031 (2005).
- 152 Baar, K. *et al.* Adaptations of skeletal muscle to exercise: rapid increase in the transcriptional coactivator PGC-1. *FASEB J* **16**, 1879-1886, doi:10.1096/fj.02-0367com (2002).